Physics – Uspekhi **62** (4) 319 – 339 (2019)

REVIEWS OF TOPICAL PROBLEMS PACS numbers: **12.39.–x**, **14.40.–n**, 11.15.Tk

Hadron physics in magnetic fields

M A Andreichikov, B O Kerbikov, Yu A Simonov

DOI: https://doi.org/10.3367/UFNe.2019.02.038526

Contents

Abstract. **We propose a new approach to exploring relativistic compound systems in an external magnetic field. A relativistic Hamiltonian that includes confinement, one-gluon exchange, and spin–spin interaction has been obtained applying the path integral formalism. The masses of the quark–antiquark states that correspond at zero magnetic field to the ρ- and π-meson and neutron mass have been calculated as a function of the magnetic field. The most interesting phenomena occur in superstrong magnetic fields on the order of $10^{18}-10^{20}$ G that emerge for a short time in peripheral collisions of relativistic heavy ions.**

Keywords: relativistic Hamiltonian of quark system, magnetic field, pseudomomentum, color Coulomb and spin–spin interactions, regularization, constituent separation method

1. Introduction

The behavior of hadrons, quarks, and atoms in strong magnetic fields (MFs) has been the focus of attention over the last few years [1–3] in connection with the generation of a superstrong MF, $eB \sim \Lambda_{\rm QCD}^2 \sim 10^{19}$ G, where e is the electron charge, B is the magnetic field induction, and $\Lambda_{\rm QCD}$ is the quantum chromodynamics (QCD) scale constant,[1] at the initial stages of relativistic heavy ion collisions at the Relativistic Heavy Ion Collider (RHIC) and Large Hadron Collider (LHC) [4–6]. Such MFs are the strongest among those created under laboratory conditions. It is predicted that a field weaker by four orders of magnitude exists on the surface of magnetars, a special class of neutron stars [7, 8]. The MF of $eB \sim \Lambda_{\rm QCD}^2$ exerts a direct influence on quark dynamics inside hadrons. The magnetic radius (Landau radius) $l_{\rm B} = (|e|B)^{-1/2} \simeq 0.45$ fm for the field of $eB \simeq 10^{19}$ G is smaller than the characteristic hadron radius. The analog of such a critical field is the 'atomic field' of $B_{\rm a} = \alpha^2 m_{\rm e}^2/|e| = 2.35 \times 10^9$ G, corresponding to the equality between magnetic and Bohr radii of the hydrogen atom: $a_{\rm B} = (\alpha m_{\rm e})^{-1}$. Electron motion in the plane normal to the MF direction becomes relativistic as the critical or Schwinger [9] magnetic field of $B_{\rm cr} = m_{\rm e}^2/|e| = \alpha^2 B_{\rm a} = 4.414 \times 10^{13}$ G is achieved. The energy spectrum in the symmetric gauge $\mathbf{A} = (1/2)\,\mathbf{B} \times \mathbf{r}$ used herein is expressed as

$$\varepsilon^2 - m^2 - p_z^2 = |e|B\left[2n_\perp + 1 + \left(|s| - \frac{es}{|e|}\right)\right] - e\sigma_z B\,, \quad (1)$$

where the MF is directed along the z-axis, $n_\perp = 0, 1, \ldots, s$ is the projection of angular momentum onto the MF direction, and $\sigma = \pm 1$ is the double spin projection onto the z-axis.

The lowest Landau level (LLL) corresponds to states with $es \geqslant 0$, $n_\perp = 0$, and $e\sigma_z > 0$. Electron motion along the MF remains nonrelativistic until the binding energy exceeds $m_{\rm e}$; therefore, the LLL has energy $\varepsilon \simeq m + p_z^2/(2m)$.

Another characteristic MF value extensively discussed in recent years concerns $B_\rho = m_\rho^2/|e| \simeq 10^{20}$ G, where m_ρ is the

[1] The relativistic system of units: $\hbar = c = 1$, $e^2 = 4\pi\alpha$ is used below, in which 1 GeV/e = 1.69×10^{20} G, 1 GeV$^2 \simeq 5.12 \times 10^{19}$ G.

M A Andreichikov (1,*), **B O Kerbikov** (1,2,3,†), **Yu A Simonov** (1,‡)
(1) National Research Center 'Kurchatov Institute', Alikhanov Institute of Theoretical and Experimental Physics, ul. B. Cheremushkinskaya 25, 117218 Moscow, Russian Federation
(2) Lebedev Physical Institute, Russian Academy of Sciences, Leninskii prosp. 53, 119991 Moscow, Russian Federation
(3) Moscow Institute of Physics and Technology (State University), Institutskii per. 9, Dolgoprudnyi, 141700 Moscow region, Russian Federation
E-mail: *andreichicov@mail.ru, † borisk@itep.ru, ‡ simonov@itep.ru

Received 14 December 2017, revised 30 January 2019
Uspekhi Fizicheskikh Nauk **189** (4) 337 – 358 (2019)
DOI: https://doi.org/10.3367/UFNr.2019.02.038526
Translated by Yu V Morozov; edited by A Radzig

ρ-meson mass. Regarding the ρ-meson as an elementary particle with the gyromagnetic ratio $g_\rho = 2$ (see below) and writing down the dispersion relation (1) yield for the LLL of a charged ρ-meson the following:

$$m^2_{\rho^\pm}(B) = m^2_{\rho^\pm}(B=0) - eB\,. \tag{2}$$

In a more detailed representation, eB should be substituted by the expression $(e_{\rho^\pm} s_z)B$, $s_z = \pm 1$ for ρ^+ and ρ^-, respectively. It follows from Eqn (2) that $m_{\rho^\pm}(B_\rho) = 0$, and the mass becomes virtual for $B > B_\rho$. The vanishing of charged ρ-meson mass suggests the possibility of forming a condensate of charged vector mesons. Formula (2) was proposed for the first time in Ref. [10], where the authors emphasized that it does not reflect the internal structure of the ρ-meson. It is worth noting that whether or not $g_\rho = 2$ requires special consideration, bearing in mind that the ρ-meson field is not the Yang–Mills field and does not possess the renormalization property. However, an overview of numerous studies dealing with this problem is beyond the scope of the present article. To be brief, the equality $g_\rho = 2$ is fulfilled with fairly good accuracy in both experiment and lattice calculations. A recent lattice computations [11] show that $g_\rho = 2.11 \pm 0.001$, the QCD sum rule gives 1.8 ± 0.3 [12] and 2.4 ± 0.4 [13], and an analysis of the BaBar experiment yields 2.1 ± 0.5 [14]. Paper [15] emphasizes the role of large radiative corrections for g_ρ.

Ten years after the publication of Ref. [10], the generation of an MF on the order of B_ρ became possible in heavy ion collisions, and ρ-meson condensate turned into the subject of numerous studies. Investigations performed by M N Chernodub and co-workers [16, 17] are worthy of special note here. Various aspects of the ρ-meson condensate problem are discussed in the literature. The authors of Ref. [18] maintain that condensation is in conflict with the Vafa–Witten theorem [19] stating that the spontaneous break of global internal symmetries, such as isotopic symmetry, is impossible in QCD type vector theories. Residual diagonal isotopic $U(1)_{I_3}$-symmetry is retained after the introduction of a constant MF along the z-axis. The appearance of condensate breaks $U(1)_{I_3}$, which must give rise to a Goldstone boson, in accordance with the Vafa–Witten theorem. The authors of Ref. [18] are of the opinion that the absence of this boson is equivalent to the absence of condensate. They argue in response to criticism offered in Ref. [20] that a massless boson becomes the longitudinal photon mode. It was shown in Ref. [21] that the condensate lacks homogeneity; therefore, its presence is at variance with the theorem. Finally, Ref. [22] proposes a weaker formulation of the Vafa–Witten theorem that allows the existence of condensate.

The vanishing of the charged ρ-meson mass in a strong MF and the condensate problem were considered in the context of lattice calculations [11, 17, 18, 23–25]. Reference [23] demonstrated the appearance of a condensate with quantum numbers of the charged ρ-meson in a strong magnetic field. On the other hand, Refs [11, 17, 24, 25] reported that the mass of $\rho^\pm$-mesons remains finite, while both the condensate and tachyon mode are absent in a strong MF. Paper [11] gave evidence that the vanishing of the charged ρ-meson mass in a strong MF is precluded by the quadratic-in-field term in the dispersion relation for the energy corresponding to magnetic dipole polarization. Combined analytical and lattice calculations reported in Ref. [25] indicate that the mass remains finite. Importantly, the common disadvantage of lattice calculations consists in the impossibility of taking account of the splitting of u and $\bar{\mathrm{d}}$ $(\bar{\mathrm{u}}, \mathrm{d})$ components in the $\rho^\pm$-meson wave function in a strong MF.

We believe that the central role in this discussion belongs to the fact that ρ-mesons have an internal structure. The Landau radius corresponding to B_ρ is only $l_\mathrm{B} \simeq 0.3$ fm. Investigations into the hadron's internal structure and spectrum in an MF amounting to B_ρ or a higher value are the key topic of the present review. The problem of the vanishing — or rather nonvanishing — of the $\rho^\pm$-meson mass was consistently solved in the aforementioned Ref. [25]. Formally, its conclusion can be confirmed by the variant of the Vafa–Witten theorem presented by Weinberg [26], according to which composite particles cannot be massless if their constituent components have a nonzero mass. Similar discussions about charged ρ-meson condensate took place in the past concerning the 'Sawidy vacuum' [27–29] or intermediate W-bosons [30, 31]. We think that a discussion of gluon or W-boson condensation is more meaningful than that of the ρ-condensate, because the respective theories are renormalizable.

The above assertions lead to the conclusion that taking account of the ρ-meson internal structure in a magnetic field higher than $B_\sigma = \sigma/|e|$, where $\sigma = 0.15-0.18$ GeV^2 is QCD string tension [32, 33], e.g., for $B \gtrsim B_\rho$, is of importance, since it ensures its stability (see Sections 5, 6, and 10). Investigations into the hadron internal structure and spectrum in an MF amounting to or exceeding B_σ are the central topic of the present review describing a new approach based on the Fock–Feynman–Schwinger representation for the quark Green's function. The method for the construction of the Green's function in the form of a continual integral in QCD is generalized to include magnetic fields. An electromagnetic field either directly affects quarks or influences the gluon structure via quark loops. The theory first developed for quark systems with a zero full electric charge is now extended to charged systems, such as $\rho^\pm$- and $\pi^\pm$-mesons. It will be shown that an arbitrary strong MF fails to cause the collapse of a quark system.

Studies on the properties of compound quantum systems in a strong MF have a long history and there is hardly a place for its detailed presentation here. We confine ourselves to mentioning a small amount of the most important research. The pioneering study by Shiff and Snyder [34] reports a solution to the issue of a hydrogen atom in a strong MF in the adiabatic approximation employed in all subsequent studies. This problem has been further developed in the last decade (see reviews [35, 36]). In quantum mechanics [37], the ground state energy of hydrogen atoms increases logarithmically with increasing B as $\varepsilon_0 = \lambda_0^2\,\mathrm{Ry}$, $\lambda_0 = \ln(B/B_\mathrm{a})$.

Recent studies have demonstrated that this observation holds true only as an estimate by order of magnitude. A more accurate result was obtained in paper [35] by equating the logarithmical derivatives of wave functions of the internal short-range and Coulomb potentials over a z range satisfying the condition $l_\mathrm{B} \ll z \ll a_\mathrm{B}$. As an MF amounts to $B \gtrsim (3\pi/\alpha)B_\mathrm{cr} \simeq 5.7 \times 10^{16}$ G, radiative corrections leading to the screening of the Coulomb potential become essential. As a result, the ground state energy turns to be 'frozen' [36–38] at $E_\infty \simeq -1.7$ keV [36]. When the proton finite radius is taken into account, the energy level is pushed upward to the binding energy value of $E'_\infty \simeq -0.65$ keV. It will be shown in Section 5 that a similar screening of the Coulomb potential of

one-gluon exchange plays an important role in meson spectrum stabilization in the strong MF responsible, inter alia, for the modification of the Zeeman effect in hydrogen atoms, e.g., a small shift in the well-known 21-cm radio line [39].

Reference [40] contains a detailed discussion of radiative and relativistic corrections to the energy levels of hydrogen-like atoms.

The formalism for solving the problem of the bound state in the MF is extremely varied. Let us consider two central points: the analytical expression for the propagator, and separation of external and internal variables in an MF. The expression for the relativistic propagator in a uniform MF was derived by Schwinger [9] using the proper time formalism introduced earlier by Fock [41]. Another well-known formula for the propagator was proposed by Ritus [42]. The studies discussed in the present review made use of the propagator in the Fock–Feynman–Schwinger representation in the form of a continual integral. The relevant data are presented in Section 4.

To calculate the spectrum of levels of a compound system in an MF, one should first of all distinguish the motion of the center of mass. Because the total momentum operator in the MF does not commute with the Hamiltonian, a pseudo-momentum or a magnetic momentum (the integral of motion for an electrically neutral system) is introduced. The definition and properties of this quantity are discussed in Section 2. Reviews [43, 44] deal with the quantum mechanics of compound systems in an MF; monographs [45, 46] describe physical processes in external electromagnetic fields.

Let us consider in brief the calculated results on hadron spectra and wave functions contained in the literature, including lattice calculations [18, 24–49]. The main conclusions based on these data reduce to the fact that the masses of a ρ^--meson with a spin projection $s_z = -1$ onto MF and a ρ^+-meson with $s_z = +1$ decrease with increasing field but do not vanish, which would correspond to the ρ-meson condensation [16]. As far as the ρ^0-meson mass is concerned, lattice calculations invariably reveal $\rho^0 - \pi^0$-mixing in the MF, which may account for the mass loss in the ρ^0-meson with $s_z = 0$ [47]. Another difficulty encountered in lattice calculations is the separation of contributions from $u\bar{u}$ and $d\bar{d}$ states to the meson structure. Our results need to be discussed and compared with lattice calculations of meson mass spectra in an MF, reported by Bali et al. [50]. Such a comparison is presented in Section 11. Here, suffice it to mention that the authors of Ref. [50] failed to observe ρ-meson condensation.

In Refs [51, 52], the dependence of meson masses on the MF strength was estimated by analytical methods. The influence of a static uniform MF on charmonium and bottomonium energy levels was explored in Ref. [51], which reported masses of different states and MF dependences of their formation probabilities. The nonrelativistic formalism was adopted, which is justified for heavy quarks, along with the pseudomomentum method (see Section 2) and the Cornell potential. Because even the application of pseudomomentum failed to fully separate the variables, the spectrum of bound states in an MF appeared to depend on the center-of-mass momentum.

The authors of paper [53] considered the influence of an MF on the constituent mass of quarks. They showed that hadron masses in an MF depend on the sum of quark masses which, in turn, depend on the sign of quantity es, where $s = +1$ if the quark spin is oriented along the MF, and $s = -1$ if it is oriented against the field. The authors of Ref. [53] regard the quark mass as the LLL energy. The trajectories of the field strength dependence of the meson mass in an MF are split in accordance with the sign of quantity es.

In Ref. [54], the problem of identifying the hadron mass in an MF was explored with the employment of the Nambu–Jona–Lasinio model [55]. Quark propagators were written out in the Ritus representation [42], and the sum of the quark loops was presented in the form of the Schwinger–Dyson equation. It was shown that the mass of a $\rho^\pm$-meson with projection $\sigma_z = \pm 1$ in the LLL approximation does not tend toward zero with growing field, but vanishes even in a moderate MF, if the highest Landau levels (up to $n = 20$) are taken into account. This result seems contradictory.

In Ref. [56], meson properties in an MF were considered in terms of Schwinger–Dyson and Bethe–Salpeter equations involving the Ritus representation for the propagator [42]. Special attention was given to the dependence of the density of meson states, which proved to be proportional to B^2. The linear potential alone was taken into consideration in quark–quark interactions. It was concluded, at variance with the above results of lattice calculations, that meson masses are virtually independent of the MF strength.

In Ref. [57], the dependence of the ρ-meson mass on a weak MF was determined on the assumption of the predominance of virtual decay $\rho \to \pi\pi$. The masses of ρ^0- and $\rho^\pm$-mesons were shown to decrease with increasing MF.

The behavior of ρ-meson masses in a growing MF at a finite temperature was explored in paper [52]. It was argued that mesons lose mass near critical temperatures as the temperature increases and gain it as the MF grows.

The layout of the review is as follows. Section 2 contains a description of the quantum mechanics of a compound system in an MF. It introduces the notion of pseudomomentum used to separate external and internal degrees of freedom. The central Sections 3 and 4 describe the constriction of the nonrelativistic Hamiltonian of the compound system with the use of the Fock–Feynman–Schwinger continual integral, taking account of the MF and confinement; also, analytical expressions for the mass spectra and wave functions of mesons and neutrons are derived. The constituent separation method is proposed in Section 4 to study the behavior of charged mesons in an MF based on the hadron wave function representation in the form of the product of wave functions of individual quarks. In addition, analytical expressions are obtained for the asymptotic form of mass spectra in the $eB \to \infty$ limit.

Section 5 is devoted to perturbative corrections arising from one-gluon exchange and spin-spin interaction. These corrections could lead to the collapse of the ground state, unless the influence of the MF on the virtual quark loops and regularization of the point spin–spin interaction are taken into consideration.

Section 6 deals with magnetic focusing. It is shown that this phenomenon causes displacement of the hydrogen 21-cm radio line in a strong MF.

Mixing and splitting of the wave functions of hadrons with different spin projections under the influence of an MF are discussed in Section 7.

Section 8 considers the influence of a strong MF on one-pion exchange, which effectively increases the hyperfine interaction constant for baryons.

Chiral effects in an MF maintaining the finite pion mass in an arbitrary strong field are dealt with in Section 9.

Section 10 contains the general statement that hadrons remain stable in arbitrary strong MFs.

Section 11 presents a detailed description of calculated data, mass versus MF plots, and their comparison with the results of lattice calculations.

In the concluding Section 12, the main results obtained for hadrons in an MF by the relativistic Hamiltonian method are summarized, and problems to be considered in the future in the framework of the given formalism are briefly discussed.

2. System of fermions in a constant uniform magnetic field

The energy levels of a spin-1/2 charged particle placed in a constant uniform magnetic field directed parallel to the z-axis and given in symmetric gauge $\mathbf{A} = (1/2)\,\mathbf{B} \times \mathbf{r}$ are found by solving the Dirac equation and are defined by formula (1).

Let us consider a system of two interacting particles with interaction potential $V(\mathbf{r}_1 - \mathbf{r}_2)$. In the absence of an MF, the particles form a bound state characterized by a discrete spectrum with respect to the coordinate $\boldsymbol{\eta} = \mathbf{r}_1 - \mathbf{r}_2$ of their relative motion, and the continuous spectrum of the free center-of-mass motion with momentum $\mathbf{P}$. As mentioned in the Introduction, the operator of the center-of-mass momentum $\mathbf{P}$ in the MF does not commute with the Hamiltonian. An electrically neutral system is significantly different from a system charged as a whole. The former has an integral of motion, i.e., a pseudomomentum [43, 44, 58–62] responsible for translational invariance of the system as a whole in the MF and describing the continuous part of the spectrum. The initial idea of the integral of motion in the MF for a single particle originates from the classical equation $\dot{\mathbf{p}} = e(\dot{\mathbf{r}} \times \mathbf{B})$. Generalization for the quantum case gives

$$\hat{\mathbf{K}} = \hat{\mathbf{p}} + e\mathbf{B} \times \hat{\mathbf{r}} = \hat{\mathbf{P}} - e\hat{\mathbf{A}} + e\mathbf{B} \times \hat{\mathbf{r}}\,, \tag{3}$$

where $\hat{\mathbf{p}}$ is the usual (kinetic) momentum, and $\hat{\mathbf{P}} = -\mathrm{i}\nabla$ is the generalized (canonical) momentum. In the quantum case, $\hat{\mathbf{K}}$ becomes the integral of motion, too, i.e., $[\hat{\mathbf{K}}, \hat{H}] = 0$, but components $\hat{K}_x$ and $\hat{K}_y$ (with MF direction $\mathbf{B} \parallel z$) cannot be diagonalized simultaneously, $[\hat{K}_x, \hat{K}_y] = -\mathrm{i}eB$. From the mathematical standpoint, the existence of $\hat{\mathbf{K}}$ follows from Hamiltonian invariance with respect to a group of magnetic translations (translational invariance of the guiding center of the Landau orbit in the MF) and the gauge group. If component K_x is diagonalized in the stationary state, the position of the guiding center of the Landau orbit is given by the expression

$$y_0 = -\frac{K_x}{eB}\,, \tag{4}$$

and the degeneracy multiplicity in the xy plane having the area $S = L_x L_y$ is given by formula

$$g = L_x \int \mathrm{d}K_x = |e|SB\,, \tag{5}$$

where L is the linear size of the system.

In the symmetric gauge $\mathbf{A}(\mathbf{r}) = (1/2)\,\mathbf{B} \times \mathbf{r}$, the pseudomomentum assumes the form

$$\hat{\mathbf{K}} = \mathbf{P} + \frac{1}{2}\,\mathbf{B} \times \mathbf{r}\,. \tag{6}$$

The notion of pseudomomentum is generalized for the case of an electrically neutral system of two or several particles in a constant uniform magnetic field. Let us consider two nonrelativistic particles with charges $e_1 = e > 0$, $e_2 = -e$ and masses m_1, m_2. The Hamiltonian lacking $\boldsymbol{\sigma}_i\mathbf{B}$ terms and spin-dependent interaction has the form

$$\hat{H} = \hat{H}_B + \hat{V} = \frac{1}{2m_1}\left(\mathbf{p}_1 - e\mathbf{A}(\mathbf{r}_1)\right)^2 + \frac{1}{2m_2}\left(\mathbf{p}_2 + e\mathbf{A}(\mathbf{r}_2)\right)^2 + V(\mathbf{r}_1 - \mathbf{r}_2)\,. \tag{7}$$

Introducing variables

$$\mathbf{R} = \frac{m_1\mathbf{r}_1 + m_2\mathbf{r}_2}{M}\,, \quad M = m_1 + m_2\,,$$

$$\mathbf{P} = \mathbf{p}_1 + \mathbf{p}_2 = -\mathrm{i}\,\frac{\partial}{\partial\mathbf{R}}\,, \quad \boldsymbol{\eta} = \mathbf{r}_1 - \mathbf{r}_2\,,$$

$$\boldsymbol{\pi} = -\mathrm{i}\,\frac{\partial}{\partial\boldsymbol{\eta}}\,, \quad \mu = \frac{m_1 m_2}{M}\,, \quad s = \frac{m_1 - m_2}{M}$$

leads in the symmetric gauge to

$$\hat{H}_B = \frac{1}{2M}\left(\mathbf{P} - \frac{e}{2}\,\mathbf{B} \times \boldsymbol{\eta}\right)^2 + \frac{1}{2\mu}\left(\boldsymbol{\pi} - \frac{e}{2}\,\mathbf{B} \times \mathbf{R} + s\,\frac{e}{2}\,\mathbf{B} \times \mathbf{r}\right)^2. \tag{8}$$

For this two-particle system the operator of pseudomomentum commuting with Hamiltonian (7), (8) has the following form in the symmetric gauge:

$$\hat{\mathbf{K}} = \sum_{i=1}^{2}\left(\mathbf{p}_i + \frac{1}{2}\,e_i\mathbf{B} \times \mathbf{r}_i\right) = \mathbf{P} + \frac{e}{2}\,\mathbf{B} \times \boldsymbol{\eta} = -\mathrm{i}\,\frac{\partial}{\partial\mathbf{R}} + \frac{e}{2}\,\mathbf{B} \times \boldsymbol{\eta}\,. \tag{9}$$

Because the pseudomomentum is the integral of motion, eigenfunctions $\Psi(\mathbf{R}, \boldsymbol{\eta})$ can be chosen so that they are eigenfunctions of all three components of operator $\hat{\mathbf{K}}$:

$$\hat{\mathbf{K}}\Psi(\mathbf{R}, \boldsymbol{\eta}) = \mathbf{K}\Psi(\mathbf{R}, \boldsymbol{\eta})\,, \tag{10}$$

where $\hat{\mathbf{K}}$ is the pseudomomentum operator, and $\mathbf{K}$ is its eigenvalue. Let us represent the wave function as $\psi(\mathbf{R}, \boldsymbol{\eta}) = \exp(\mathrm{i}\boldsymbol{\nu}\mathbf{R})\varphi(\boldsymbol{\eta})$ with the yet unknown vector $\boldsymbol{\nu}$. Then, one obtains

$$\hat{\mathbf{K}}\Psi(\mathbf{R}, \boldsymbol{\eta}) = \left(\boldsymbol{\nu} + \frac{e}{2}\,\mathbf{B} \times \mathbf{r}\right)\exp(\mathrm{i}\boldsymbol{\nu}\mathbf{R})\varphi(\boldsymbol{\eta}) = \mathbf{K}\exp(\mathrm{i}\boldsymbol{\nu}\mathbf{R})\varphi(\boldsymbol{\eta})\,. \tag{11}$$

Hence, $\boldsymbol{\nu}$ is found and we got $\Psi(\mathbf{R}, \boldsymbol{\eta})$ in the form

$$\Psi(\mathbf{R}, \boldsymbol{\eta}) = \exp\left[\mathrm{i}\left(\mathbf{K} - \frac{e}{2}\,\mathbf{B} \times \boldsymbol{\eta}\right)\mathbf{R}\right]\varphi(\boldsymbol{\eta})\,. \tag{12}$$

Using formula (12), the equation $\hat{H}\Psi = E\Psi$ is reduced to the equation for $\varphi(\boldsymbol{\eta})$:

$$\left[\frac{\mathbf{K}^2}{2M} - \frac{e}{M}(\mathbf{K} \times \mathbf{B})\boldsymbol{\eta} + \frac{\boldsymbol{\pi}^2}{2\mu} + \frac{e^2}{8\mu}(\mathbf{B} \times \boldsymbol{\eta})^2 - \frac{e}{2}\,\frac{s}{\mu}\mathbf{B}(\boldsymbol{\eta} \times \boldsymbol{\pi}) + V(\boldsymbol{\eta})\right]\varphi_K(\boldsymbol{\eta}) = E\varphi_K(\boldsymbol{\eta})\,. \tag{13}$$

A complete separation of variables $\mathbf{R}$ and $\boldsymbol{\eta}$ fails to occur, because the second item in equation (13) relates the motion of the center of mass to the internal motion. The relationship has the form of an electrostatic potential of the electric field $(\mathbf{K}_\perp \times \mathbf{B})/M$, where $\mathbf{K}_\perp = K_x \boldsymbol{\eta}_x + K_y \boldsymbol{\eta}_y$, and the MF is directed along the z-axis. In other words, the Stark effect takes place owing to the motion of the center of mass. The relationship between internal and external variables is reminiscent of the influence of electron angular motion in a hydrogen atom on the radial motion due to item $l(l+1)$.

Equation (13) allows an analytical solution for the oscillator potential. Consideration of this case is of importance for further discussions, because the oscillatory approximation for quark–quark interaction will be used at the first stage of the study of the MF strength dependence of the meson mass.

Let us choose this potential in the form

$$V(\mathbf{r}) = \frac{\sigma}{2\gamma}\,\mathbf{r}^2 + \frac{\sigma\gamma}{2}\,;$$

its subsequent minimization in parameter γ reproduces the linear potential in the range of values being considered with a 5% accuracy. (In this section, we omit the additive parameter $\sigma\gamma/2$ that will be considered later in Section 4). Quark masses are assumed to be identical: $m_1 = m_2 = m$, and the orbital moment l of the relative motion equal to zero. In this case, energy levels are expressed as

$$E(\mathbf{K}, n_\perp, n_z, l) = 2\Omega(2n_\perp + 1) + \omega\left(n_z + \frac{1}{2}\right) + \frac{1}{4m}\left[\frac{K_x^2 + K_y^2}{1 + \gamma e^2 B^2/(2\sigma m)} + K_z^2\right], \tag{14}$$

$$\Omega = \frac{eB}{m}\sqrt{1 + \frac{2\sigma m}{\gamma e^2 B^2}}, \qquad \omega = \sqrt{\frac{\sigma}{2\gamma m}}. \tag{15}$$

It follows from formula (14) that the ground state for the oscillator potential matches the state with $\mathbf{K} = 0$.

Let us briefly touch upon the separation of variables and pseudomomentum for a system of three particles (neutrons are meant) [44, 63], two with charges $-e/3$ and coordinates $\mathbf{r}_1$ and $\mathbf{r}_2$, respectively, the third having charge $2e/3$ and coordinate $\mathbf{r}_3 (e > 0)$. The sum of their masses is designated as $m_+ = 2m + m_3$. Let us further choose (as before) the symmetric gauge of the MF and introduce the Jacobi coordinates with the respective conjugate momenta:

$$\boldsymbol{\eta} = \frac{\mathbf{r}_1 - \mathbf{r}_2}{\sqrt{2}}\,, \quad \boldsymbol{\xi} = \sqrt{\frac{m_{\mathrm{u}}}{2M}}(\mathbf{r}_1 + \mathbf{r}_2 - 2\mathbf{r}_3), \quad \mathbf{R} = \frac{1}{M}\sum_{i=1}^{3} m_i\,\mathbf{r}_i\,. \tag{16}$$

$$\boldsymbol{\pi} = -\mathrm{i}\frac{\partial}{\partial\boldsymbol{\eta}}, \quad \mathbf{q} = -\mathrm{i}\,\frac{\partial}{\partial\boldsymbol{\xi}}, \quad \mathbf{P} = -\mathrm{i}\,\frac{\partial}{\partial\mathbf{R}}\,. \tag{17}$$

The pseudo-momentum of such a system has the form

$$\hat{\mathbf{K}} = \mathbf{P} - \frac{e}{2}\sqrt{\frac{M}{2m_3}}\,\mathbf{B} \times \boldsymbol{\xi}\,. \tag{18}$$

Calculations similar to those that have led from Eqn (7) to Eqn (13) yield the following expressions for the Hamiltonian in the external MF, but without interaction between particles, and for $\mathbf{K} = 0$:

$$\hat{H}_B = -\frac{1}{2m}(\Delta_\xi + \Delta_\eta) + \frac{1}{2m}\left(\frac{eB}{4}\right)^2\left[\frac{m_+^2}{m_3^2}(\boldsymbol{\xi}_\perp)^2 + (\boldsymbol{\eta}_\perp)^2\right] + \frac{eB}{4m}\left(\frac{m_3 - 2m}{m_3}\,\mathbf{L}^{(\xi)} + \mathbf{L}^{(\eta)}\right). \tag{19}$$

Here, $\mathbf{L}^{(\xi)}$ and $\mathbf{L}^{(\eta)}$ are the orbital momenta in terms of the respective Jacobi coordinates commuting with each other. In Section 5, formulas (18) and (19) will be utilized to explore the MF strength dependence of the neutron mass.

The above procedure of separating the variables proves impossible in a charged system. The formal introduction of a pseudo-momentum does not ensure simultaneous diagonalization of components K_x and K_y, as in the case of a single charged particle. The center of mass of the charged system loses translational invariance and precesses in the plane perpendicular to the MF direction with frequency $\Omega = (e_1 + e_2)B/\,(m_1 + m_2)$. The motion of the center of mass is not confined to trivial precession, the internal and external degrees of freedom remaining inseparable. The motion of the center of mass gives rise to an oscillating electric field, and the system as a whole moves in a fairly complicated way [64]. Separation of variables is possible only in a system with equal masses, $m_1 = m_2$ [65]. Its impossibility in a charged system makes necessary the search for approximate methods to solve the problem. The authors of Ref. [25] proposed the constituent separation technique, with the zero-order approximation describing the totality of noninteracting particles (see Section 4).

3. Relativistic formalism for a quark system in a magnetic field

This section is designed to introduce the reader to the general relativistic formalism allowing a description of systems with quantum-electrodynamic (QED) and quantum-chromodynamic (QCD) interactions in an external MF in terms of the relativistic Hamiltonian (RH). The proposed approach is applicable to a large class of systems, including atoms, molecules, nuclei, and hadrons placed in an arbitrarily strong magnetic field. To recall, a strong MF not only affects charged constituents but also changes the interaction kernel itself. Moreover, the ability of a strong MF to make a vacuum unstable should be borne in mind. These circumstances impose limitations on the application of the Bethe–Salpeter method, because the nonperturbative QCD interaction cannot be described in terms of the perturbation theory by the totality of exchange diagrams. Moreover, enhanced interaction in the context of the Bethe–Salpeter equation in the relativistic theory leads to collapse [66]. The path integral method proposed in paper [67] and further developed in Refs [68–72] permits avoiding the said issues and consistently solving the problem of finding spectrum and wave functions.

In the approach under consideration, the interaction between components of a compound system is introduced using relativistic and gauge-invariant Wilson loop formalisms. Let us begin with a consideration of the one-particle Green's function of fermion in 4D Euclidean space [73]:

$$S(x, y) = (m + \hat{D})^{-1}_{xy}\,, \qquad \hat{D} = \hat{\partial} - \mathrm{i}g\hat{A} - \mathrm{i}e\hat{A}^{(\mathrm{e})}\,, \tag{20}$$

where $A_\mu = (\lambda^a/2)\, A_\mu^a$ $(a = 1, 2, \ldots, 8)$, $A_\mu^{(\mathrm{e})}$ are the vector potentials of gluon and electromagnetic fields, respectively. Let us then determine the scalar Green's function $G(x, y)$ with the aid of the Dirac projection operator according to the relation $S(x, y) = (m - \hat{D})G(x, y)$. Function $G(x, y)$ can be represented as the continual integral (Fock–Feynman–Schwinger representation, FFSR) [70]:

$$G(x, y) = \left(\frac{1}{m^2 - D_\mu^2}\right)_{xy} = \int_0^\infty \mathrm{d}s\, (D^4 z)_{xy} \exp(-K)\Phi(x, y)\Phi_\sigma(x, y)\,, \quad (21)$$

where K is the kinetic kernel:

$$K = m^2 s + \frac{1}{4}\int_0^s \mathrm{d}\tau \left(\frac{\mathrm{d}z_\mu}{\mathrm{d}\tau}\right)^2, \quad (22)$$

and Φ and Φ_σ are dynamic kernels:

$$\Phi(x, y) = P_A \exp\left(\mathrm{i}g \int_y^x (gA_\mu + eA_\mu^{(\mathrm{e})})\, \mathrm{d}z_\mu\right),$$
$$\Phi_\sigma(x, y) = P_F \exp\left(\int_0^s \mathrm{d}\tau\, \sigma_{\mu\nu}(gF_{\mu\nu} + eB_{\mu\nu})\right). \quad (23)$$

Here, $(D^4 z)_{xy}$ is the measure of integration encompassing all paths and connecting points y and x in the 4D Euclidean space, P_A and P_F are path and surface ordering operators, respectively, because A_μ and $F_{\mu\nu}$ contain color matrices, and $\sigma_{\mu\nu}F_{\mu\nu}$ and $\sigma_{\mu\nu}B_{\mu\nu}$ are 4×4 Dirac matrices, $\sigma_{\mu\nu} = (\gamma_\mu\gamma_\nu - \gamma_\nu\gamma_\mu)/(4\mathrm{i})$, for example

$$\sigma_{\mu\nu}F_{\mu\nu} = \begin{pmatrix} \boldsymbol{\sigma}\mathbf{H} & \boldsymbol{\sigma}\mathbf{E} \\ \boldsymbol{\sigma}\mathbf{E} & \boldsymbol{\sigma}\mathbf{H} \end{pmatrix}. \quad (24)$$

An important difference between the relativistic continual integral (22) and the nonrelativistic analog is as follows. In quantum mechanics, the measure of integration has the form $D^3 z = D^3 z(t)$, and time t plays the role of an order parameter, since sequential sections of trajectory $\mathbf{z}(t)$ are ordered in time. In the relativistic path integral, this role is played by monotonically growing proper time τ, while $z_4(\tau)$ contains monotone $(\bar{z}_4(\tau))$, and fluctuating $(\tilde{z}_4(\tau))$ components, i.e., $z_4(\tau) = \bar{z}_4(\tau) + \tilde{z}_4(\tau)$. Evidently, $\tilde{z}_4(\tau)$ corresponds to the part of the trajectory that is called the Z-graph and contains $\mathrm{e}^+\mathrm{e}^-$- and $\mathrm{q}\bar{\mathrm{q}}$-pair production. These trajectories need to be considered in order e^4 for QED and g^4 for QCD. Ignoring this effect in the first order allows time $\bar{z}_4(\tau)$ to be regarded as proportional to τ: $\bar{z}_4(\tau) = 2\omega\tau \equiv t_\mathrm{E}$. Quantity ω is related in a similar way to the total self-time s in accordance with the formula $s = T/(2\omega)$, where T is the total Euclidean time: $T = |x_4 - y_4|$. As a result, Green's function (21) takes the following form (with Φ_σ omitted for simplicity):

$$G(x, y) = (m^2 - \hat{D}^2)^{-1}_{xy} = T\int_0^\infty \frac{\mathrm{d}\omega}{2\omega^2}\, (D^3 z)_{xy} \exp\big(-K(\omega)\big)\big\langle \Phi(x, y)\big\rangle\,, \quad (25)$$

where

$$K(\omega) = \int_0^T \mathrm{d}t_\mathrm{E} \left[\frac{\omega}{2} + \frac{m^2}{2\omega} + \frac{\omega}{2}\left(\frac{\mathrm{d}\bar{z}}{\mathrm{d}t_\mathrm{E}}\right)^2\right], \quad (26)$$

and $\langle\Phi(x, y)\rangle = \int Dz_4 \Phi(x, y)$ is expressed (disregarding fluctuations) as

$$\langle\Phi(x, y)\rangle = \sqrt{\frac{\omega}{2\pi T}} \exp\left\{\mathrm{i}\int_y^x \left[eA_\mu^{(\mathrm{e})}(\bar{z}, t_\mathrm{E}) + gA_\mu(\bar{z}, t_\mathrm{E})\right] \mathrm{d}z_\mu\right\}, \quad (27)$$

where $\mathrm{d}z_\mu = (\mathrm{d}z_i, \mathrm{d}t_\mathrm{E})$. This representation of Green's function of a quark–antiquark pair looks like

$$G_1(x, y)G_2(x, y) = \frac{T}{8\pi}\int_0^\infty \frac{\mathrm{d}\omega_1}{\omega_1^{3/2}}\int_0^\infty \frac{\mathrm{d}\omega_2}{\omega_2^{3/2}}\, (D^3 z_1)_{xy}(D^3 z_2)_{xy} \exp\big(-A(W)\big)\langle W\rangle\,, \quad (28)$$

where $A = K_1(\omega_1) + K_2(\omega_2)$, and $\langle W\rangle$ is the Wilson loop containing electromagnetic and gluon fields:

$$\big\langle W(A, A^{(\mathrm{e})})\big\rangle = \left\langle P\exp\left[\mathrm{i}\oint (eA_\mu^{(\mathrm{e})} + gA_\mu)\, \mathrm{d}z_\mu\right]\right\rangle. \quad (29)$$

In what follows, the term electromagnetic fields means the external uniform MF $A_\mu^{(\mathrm{e})} = (\mathbf{A}_\mu^{(\mathrm{e})}, 0)$; averaging is performed over vacuum fields A_μ with the nonzero correlator $F_{\mu\nu}$. The relationship between Wilson loop averaging and the potential is well known [74]. Setting up our problem in the Gaussian approximation [32] yields [67, 75–79]

$$\langle W\rangle = Z_W \exp\left[-\int V_0\big(r(t_\mathrm{E})\big)\, \mathrm{d}t_\mathrm{E}\right], \quad (30)$$

where $r(t_\mathrm{E}) = |\bar{z}_1(t_\mathrm{E}) - \bar{z}_2(t_\mathrm{E})|$, and $V_0(r)$ is the sum of the nonperturbative confinement potential and the one-gluon exchange (OGE) contribution:

$$V_0(r) = V_\mathrm{conf}(r) + V_\mathrm{OGE}(r)\,, \quad (31)$$

where V_conf and V_OGE are expressed through the Gaussian correlators of stochastic color fields:

$$V_\mathrm{conf}(r) = 2r\int_0^r \mathrm{d}\lambda \int_0^\infty \mathrm{d}\nu\, D(\lambda, \nu) \to \sigma r\,, \quad r \to \infty\,, \quad (32)$$

$$V_\mathrm{OGE}(r) = \int_0^r \lambda\, \mathrm{d}\lambda \int_0^\infty \mathrm{d}\nu\, D_1(\lambda, \nu) = -\frac{4}{3}\frac{\alpha_\mathrm{s}}{r}\,, \quad (33)$$

$$\sigma = 2\int_0^\infty \mathrm{d}\nu \int_0^\infty \mathrm{d}\lambda\, D(\lambda, \nu)\,, \quad (34)$$

where α_s is the strong interaction constant, and σ is the string tension of the linear confinement potential. Scalar functions D and D_1 are included in the representation for the gluon field quadratic cumulant (correlator) [32, 78, 79]:

$$D_{\mu\nu\lambda\sigma}(x, y) \equiv g^2 \frac{1}{N_\mathrm{c}}\, \mathrm{tr}\,\big\langle F_{\mu\nu}(x)\Phi F_{\lambda\sigma}(y)\Phi\big\rangle = (\delta_{\mu\lambda}\delta_{\nu\sigma} - \delta_{\mu\sigma}\delta_{\nu\lambda})D(x - y) + \frac{1}{2}\,\partial_\mu\Big\{\big[(h_\lambda\delta_{\nu\sigma} - h_\sigma\delta_{\nu\lambda}) + (\mu\lambda \leftrightarrow \nu\sigma)\big]D_1(x - y)\Big\}\,, \quad (35)$$

where $h_\mu \equiv x_\mu - y_\mu$, N_c is the number of colors. At the concluding stage, Green's function presented in the form of the path integral can be written out using the evolution operator. By way of example, for a single particle in the absence of an external field, one obtains

$$\int (D^3 z)_{xy} \exp\big(-K(\omega)\big) = \langle x|\exp\big(-H(\omega)T\big)|y\rangle\,, \quad (36)$$

where $H(\omega)$ is the relativistic Hamiltonian of a free particle: $H(\omega) = (\mathbf{p}^2 + m^2)/(2\omega) + \omega/2$. The main focus in this review being the characteristic of hadron ground states in an MF at different orientations of quark magnetic moments in the $T \to \infty$ limit, integrals over ω in expressions (25) and (28) can be calculated by the stationary phase method, i.e., under conditions of satisfying the equality

$$\left.\frac{\partial H(\omega)}{\partial \omega}\right|_{\omega=\omega_0} = 0\,. \tag{37}$$

Therefore, one finds for a free relativistic particle: $\omega_0 = \sqrt{\mathbf{p}^2 + m^2}$, $H(\omega_0) = \sqrt{\mathbf{p}^2 + m^2}$. The Green's function of the quark–antiquark system in an external MF (28) can be expressed, by analogy with formula (36), in the form

$$G_1(x,y)G_2(x,y) = \frac{T}{8\pi}\int_0^\infty \frac{\mathrm{d}\omega_1}{\omega_1^{3/2}}\int_0^\infty \frac{\mathrm{d}\omega_2}{\omega_2^{3/2}}\,\langle x|\exp\left[-H(\omega_1,\omega_2,\mathbf{p}_1,\mathbf{p}_2)T\right]|y\rangle\,. \tag{38}$$

The Hamiltonian in Eqn (38) includes potential V_0 defined in Eqn (31). In the symmetric gauge, taking into account that $\int \mathrm{d}\tau\,\sigma_{\mu\nu}B_{\mu\nu} = \int \mathrm{d}t_{\mathrm{E}}/(2\omega)\boldsymbol{\sigma}\mathbf{B}$, we arrive at

$$\hat{H} = \sum_{i=1}^{2}\left[\left(\frac{\mathbf{p}_i - (e_i/2)(\mathbf{B}\times\mathbf{r}_i)}{2\omega_i}\right)^2 + \frac{\omega_i^2 + m_i^2 - e_i\,\boldsymbol{\sigma}_i\mathbf{B}}{2\omega_i}\right] + V_0(\mathbf{r}) \equiv H_B + H_\sigma + V_0(\boldsymbol{\eta})\,, \tag{39}$$

where H_B and H_σ denote the first and second terms beneath the summation sign.

The entire nonperturbative meson dynamics are contained in Hamiltonian (39). To calculate the ground state mass, it is necessary to distinguish in the Green's function the projection onto the space of internal degrees of freedom, i.e., to perform the following integration in formula (38):

$$\int \mathrm{d}^3(x-y)\,\langle x|\exp\left[-H(\omega_1,\omega_2,\mathbf{p}_1,\mathbf{p}_2)T\right]|y\rangle = \sum_n \varphi_n^2(\boldsymbol{\eta})\exp\left[-M_n(\omega_1,\omega_2)T\right]\,, \tag{40}$$

where $\varphi_n(\boldsymbol{\eta})$ is the wave function of an internal motion. The ground state mass M_0 may be found by computing integral (38) using the stationary phase technique. Therefore, the nonperturbative or dynamic mass is given by the following set of equations

$$\hat{H}|\varphi_0\rangle = M_0(\omega_1,\omega_2)|\varphi_0\rangle\,, \tag{41}$$

$$\left.\frac{\partial M_0}{\partial \omega_i}\right|_{\omega_i=\omega_i^{(0)}} = 0, \qquad i = 1,2\,. \tag{42}$$

A detailed discussion of the solution to the Hamiltonian (39) spectrum issue is presented in Section 4. The total mass M_{tot} is the sum of the nonperturbative mass M_0 corresponding to the ground state of Hamiltonian (39) and perturbative corrections of three types:

$$M_{\mathrm{tot}} = M_0 + \Delta M_{\mathrm{OGE}} + \Delta M_{\mathrm{SS}} + \Delta M_{\mathrm{SE}}\,. \tag{43}$$

Here, $\Delta M_{\mathrm{OGE}} = \langle\varphi_0|\hat{V}_{\mathrm{OGE}}|\varphi_0\rangle$ is the contribution from one-gluon exchange, ΔM_{SS} arises from color-magnetic spin–spin interaction, and ΔM_{SE} is the contribution from the quark self-energy.

All three summands will be considered in Section 6. Here, suffice it to mention that one-gluon exchange and spin–spin interaction may be responsible for emerging the spectrum instability (fall on attracting center).

4. Methods for calculating hadron spectra in a magnetic field

It was shown in Section 2 that the problem of an electrically neutral system placed in an MF allows quasiseparation of external and internal variables to be implemented. The spectrum of Hamiltonian (7) energy levels is given by equation (13) owing to the introduction of pseudomomentum. The relativistic analog of formula (7) is Hamiltonian (39), obtained in Section 3, which depends on quark 'dynamic masses' ω_i. In a relativistic case, expression (8) should be replaced by

$$\hat{H}_B = \frac{1}{2(\omega_1+\omega_2)}\left[\mathbf{P} - \frac{e}{2}(\mathbf{B}\times\boldsymbol{\eta})\right]^2 + \frac{1}{2\tilde{\omega}}\left[\boldsymbol{\pi} - \frac{e}{2}(\mathbf{B}\times\mathbf{R}) + \frac{e}{2}\,s\mathbf{B}\times\boldsymbol{\eta})\right]^2. \tag{44}$$

The quantities entering this formula are defined in Section 2 within the accuracy of $m_i \to \omega_i$, $\mu \to \tilde{\omega}$ substitutions. Following the formalism set forth in Section 2 (formulas (9)–(13)), we introduce the pseudomomentum and arrive at the equation for the wave function $\varphi_K(\boldsymbol{\eta})$ of internal motion:

$$\left\{\frac{1}{2(\omega_1+\omega_2)}\left[\mathbf{K} - e(\mathbf{B}\times\boldsymbol{\eta})\right]^2 + \frac{1}{2\tilde{\omega}}\left[\boldsymbol{\pi} + \frac{e}{2}\,s(\mathbf{B}\times\boldsymbol{\eta})\right]^2 + V_0(\boldsymbol{\eta})\right\}\varphi_K(\boldsymbol{\eta}) = \varepsilon(\omega_1,\omega_2)\varphi_K(\boldsymbol{\eta})\,. \tag{45}$$

It follows from nonrelativistic formula (13) and its relativistic analog (45) that the center-of-mass motion affects the internal motion owing not only to the term $\mathbf{K}^2/2(\omega_1+\omega_2)$, but also (which is more important) to the expression $(\mathbf{K}\times\mathbf{B})\boldsymbol{\eta}/(\omega_1+\omega_2)$. Due to this, the wave function $\varphi_K(\boldsymbol{\eta})$ has subscript K. The analytical solution of equation (45) gives the explicit physical picture. The first step is separation of motion in the plane perpendicular to the field and along the MF direction. Function $\varphi_K(\boldsymbol{\eta})$ can be represented as follows [58–62]:

$$\varphi_K(\boldsymbol{\eta}) = \exp\left(-\mathrm{i}\,\frac{s}{2}\,\mathbf{K}_\perp\boldsymbol{\eta}\right)\varphi'_K(\boldsymbol{\eta}')\,, \tag{46}$$

where

$$\mathbf{K}_\perp = \mathbf{e}_x K_x + \mathbf{e}_y K_y\,, \quad \boldsymbol{\eta}' = \boldsymbol{\eta} - \boldsymbol{\eta}_0\,, \quad \boldsymbol{\eta}_0 = -\frac{\mathbf{K}\times\mathbf{B}}{eB^2}\,. \tag{47}$$

Substituting expressions (46) and (47) into (45) yields the equation

$$\left[\frac{K_z^2}{2(\omega_1+\omega_2)} - \frac{1}{2\tilde{\omega}}\frac{\partial^2}{\partial\eta_z'^2} - \frac{1}{2\tilde{\omega}}\left(\frac{\partial^2}{\partial\eta_x'^2} + \frac{\partial^2}{\partial\eta_y'^2}\right) - \frac{eB}{2}\frac{s}{\tilde{\omega}}l_z' + \frac{e^2B^2}{8\tilde{\omega}}(\eta_x'^2 + \eta_y'^2)\right]\varphi'_K(\boldsymbol{\eta}') = \varepsilon(\omega_1,\omega_2)\varphi'_K(\boldsymbol{\eta}')\,. \tag{48}$$

The transverse part of equation (48) describes the Landau levels of a charged particle in an MF [37] with the center displaced by $\boldsymbol{\eta}_0$ due to the effective electric field acting on internal variables. We are interested in meson ground states and therefore assume $l_z' = 0$ in equation (48). Then, for eigenvalues $\varepsilon(\omega_1, \omega_2)$ one obtains

$$\varepsilon(\omega_1, \omega_2) = \frac{K_z^2}{2(\omega_1 + \omega_2)} + \frac{p_z^2}{2\tilde{\omega}} + \frac{eB}{2\tilde{\omega}}(2n_\rho + 1)\,, \tag{49}$$

where $\rho^2 = \eta_x'^2 + \eta_y'^2$, $n_\rho = 0, 1, 2, \ldots$. Notice that expression (49) does not reduce to the sum of eigenenergies of two unrelated particles at Landau levels with zero orbital momentum:

$$\varepsilon'(\omega_1, \omega_2) = \frac{p_{z1}^2}{2\omega_1} + \frac{eB}{2\omega_1}(2n_{\rho 1} + 1) + \frac{p_{z2}^2}{2\omega_2} + \frac{eB}{2\omega_2}(2n_{\rho 2} + 1)\,. \tag{50}$$

Evidently, formulas (49) and (50) give equivalent spectra and similar degrees of state degeneracy.

Let us turn to the solution of the problem of finding the spectrum of Hamiltonian (39), including Hamiltonian (44) as a constituent component. The problem with the linear confinement potential $V_0(\boldsymbol{\eta}) = V_{\text{conf}}(\eta) = \sigma\eta$, $\sigma = 0.18\ \text{GeV}^2$ [80] has only a numerical solution. Therefore, we use the confinement potential representation in the quadratic form. The accuracy of this method for calculating eigenvalues amounts to about 5% [80]. In the substitution

$$V_0(\boldsymbol{\eta}) = \sigma\eta \to \frac{\sigma}{2}\left(\frac{\eta^2}{\gamma} + \gamma\right), \tag{51}$$

γ is the positive variation parameter. Minimization of formula (51) over γ leads back to the initial confinement potential, and the assumption of zero orbital momentum to the search for eigenvalues and eigenfunctions of the Hamiltonian

$$\hat{H} = \hat{H}_B + \frac{\sigma}{2\gamma}\,\boldsymbol{\eta}^2 + \frac{\sigma\gamma}{2} + \sum_{i=1}^{2} \frac{\omega_i^2 + m_i^2 - e_i\boldsymbol{\sigma}_i\mathbf{B}}{2\omega_i}\,. \tag{52}$$

Expression (46) should be replaced by [62]

$$\varphi_K(\boldsymbol{\eta}) = \exp\left(-\mathrm{i}\,\frac{s}{2}\,\alpha\mathbf{K}_\perp\boldsymbol{\eta}\right)\chi_k(\mathbf{r})\,, \tag{53}$$

where

$$\alpha = \left(1 + \frac{(\omega_1 + \omega_2)\sigma}{\gamma e^2 B^2}\right)^{-1}, \qquad \mathbf{r} = \boldsymbol{\eta} - \alpha\boldsymbol{\eta}_0 = \left(\eta_x + \frac{\alpha}{eB}\,K_y,\quad \eta_y - \frac{\alpha}{eB}\,K_x, \eta_z\right), \tag{54}$$

and $\boldsymbol{\eta}_0$ is defined by formula (47). Substituting expression (53) into equation $\hat{H}\varphi_K(\boldsymbol{\eta}) = M\varphi_K(\boldsymbol{\eta})$ yields, after simple calculations, the result for eigenvalues:

$$M_{K,n_\perp,n_z}(\omega_1, \omega_2, \gamma) = \frac{1}{2\tilde{\omega}}\left[eB\sqrt{1 + \frac{4\sigma\tilde{\omega}}{\gamma e^2 B^2}}(2n_\rho + 1) + \sqrt{\frac{4\sigma\tilde{\omega}}{\gamma}}\left(n_z + \frac{1}{2}\right)\right] + \sum_{i=1}^{2} \frac{\omega_i^2 + m_i^2 - e_i\boldsymbol{\sigma}_i\mathbf{B}}{2\omega_i} + \frac{\sigma\gamma}{2} + \frac{1}{2(\omega_1 + \omega_2)}\left[K_z^2 + K_\perp^2(1 - \alpha)\right]. \tag{55}$$

We are interested in the masses of ground states with $n_\rho = n_z = 0$. It follows from formula (55) that the minimal M value corresponds to $K = 0$. It is a peculiar feature of oscillator potential V_{conf}. The dependence of eigenvalues on the magnitude of pseudomomentum is discussed in detail in Ref. [49]. An important property of the oscillator approximation is the simple relationship between the mean value of the system's kinetic momentum $\mathbf{P} = \sigma_j(-\mathrm{i}\boldsymbol{\nabla}_j - e_j\mathbf{A}_j)$ and the pseudomomentum value [49]:

$$\langle\mathbf{P}\rangle = \left(\frac{4K_x}{1 + \gamma e^2 B^2/(4\sigma\tilde{\omega})}\,,\ \frac{4K_y}{1 + \gamma e^2 B^2/(4\sigma\tilde{\omega})}\,,\ K_z\right). \tag{56}$$

Because formula (55) always contains $\alpha < 1$, the ground state meson in the oscillator approximation remains at rest by virtue of expression (56). The wave function of the ground state with $n_\perp = n_z = 0$, $K = 0$, and, accordingly, $\mathbf{r} = \boldsymbol{\eta}$ has the form

$$\varphi(\boldsymbol{\eta}) = \frac{1}{\sqrt{\pi^{3/2} r_\perp^2 r_z}} \exp\left(-\frac{\eta_\perp^2}{2r_\perp^2} - \frac{\eta_z^2}{2r_z^2}\right), \tag{57}$$

$$r_\perp = \sqrt{\frac{2}{|e|B}}\left(1 + \frac{4\sigma\tilde{\omega}}{\gamma e^2 B^2}\right)^{-1/4}, \quad r_z = \left(\frac{\gamma}{\sigma\tilde{\omega}}\right)^{1/4}. \tag{58}$$

As was mentioned in the Introduction, the influence of the MF is determined by the dimensionless parameter eB/σ. In relation to the hadron spectrum problem in an MF, the field will be referred to as weak if $eB/\sigma \ll 1$ (i.e., $eB \ll 10^{19}$ G), and strong if $eB/\sigma \gg 1$. It can be shown [80] that $r_\perp \approx \sqrt{2/(|e|B)}$, $r_z \approx 1/\sqrt{\sigma}$ in the strong field, and the meson wave function takes the form of an oblong ellipsoid, the size of which along the z-axis is limited by string tension, whereas there is no such limitation in the case of a hydrogen atom. A comparison of formulas (49) and (55) shows that, in the strong field limit, the energy spectrum responsible for the motion in the plane normal to the magnetic field has the form of Landau energy levels $\varepsilon(n_\perp) = [eB/(2\tilde{\omega})](2n_\perp + 1)$. As shown above, the spectrum of levels (49) is equivalent to the sum of eigenvalues of two independent particles at the Landau levels in an MF. This observation provides a basis for the constituent separation (CS) method, whose central idea is considered in this section below. The relationship between the motion in the plane perpendicular to the MF and that along the field arises in the case of simultaneous minimization of $M(\omega_1, \omega_2, \gamma)$ over all three parameters. In a weak field, $eB/\sigma \ll 1$, the MF dependence of the energy is defined by the term $e_i\boldsymbol{\sigma}_i\mathbf{B}$ in expression (55), i.e., by the interaction of quark magnetic moments with the MF.

Thus, we have calculated the spectrum and found wave functions of Hamiltonian (41). The dynamic mass of the ground state is expressed as

$$M(\omega_1, \omega_2, \gamma) = \frac{1}{2\tilde{\omega}}\left[eB\sqrt{1 + \frac{4\sigma\tilde{\omega}}{\gamma e^2 B^2}} + \sqrt{\frac{\sigma\tilde{\omega}}{\gamma}}\right] + \sum_{i=1}^{2} \frac{\omega_i^2 + m_i^2 - e_i\boldsymbol{\sigma}_i\mathbf{B}}{2\omega_i} + \frac{\sigma\gamma}{2}\,, \tag{59}$$

while the wave functions have the oscillator form (57), (58).

According to expression (46), the total meson mass is the sum of the dynamic mass (59) and perturbative corrections ΔM_{OGE}, ΔM_{SS}, and ΔM_{SE} (see Section 5).

Let us consider the neutron dynamic mass in an MF [81] making use of nonrelativistic Hamiltonian (19) obtained in

Section 2 for three particles in the MF. First of all, we substitute $m_i \to \omega_i$ and assume orbital momenta in the ground state to be zero. Then, we add items describing the interaction between quark magnetic moments and the MF, confinement, color Coulomb interaction, and spin–spin forces. This leads to the following Hamiltonian for a neutron:

$$\hat{H}_{\mathrm{N}} = \hat{H}_{\mathrm{B}} + V_\sigma + V_{\mathrm{conf}} + V_{\mathrm{OGE}} + V_{\mathrm{SS}} + \Delta M_{\mathrm{SE}}\,, \tag{60}$$

where $\hat{H}_B$ is derived from expression (19) by means of the above substitution, and the potentials take the form

$$V_\sigma = -\sum_{i=1}^{3} \frac{e_i \boldsymbol{\sigma}_i \mathbf{B}}{2\omega_i}, \quad V_{\mathrm{conf}} = \sigma \sum_{i=1}^{3} |\mathbf{x}_i - \mathbf{x}_{\mathrm{Y}}|\,. \tag{61}$$

Coordinate $\mathbf{x}_{\mathrm{Y}}$ corresponds to the string branch point (Torricelli point). The fact that three quarks in a baryon form the so-called Y-configuration emerges from the explicit calculation by the method in question [33] and is confirmed by lattice calculations [82–84]. Expressions for the contributions from one-gluon exchange and the self-energy part are analogous to the respective quantities for mesons. The confinement potential is approximated by the oscillator expression

$$\begin{aligned} V_{\mathrm{conf}} &= \sigma \sum_{i=1}^{3} |\mathbf{x}_i - \mathbf{x}_{\mathrm{Y}}| \to 3\,\frac{\sigma\gamma}{2} + \frac{\sigma}{2\gamma} \sum_{i=1}^{3} (\mathbf{x}_i - \mathbf{x}_{\mathrm{Y}})^2 \\ &\to \frac{3\sigma\gamma}{2} + \frac{\sigma}{2\gamma}\left(\frac{\omega_3^2 + 2\omega^2}{\omega_+\omega_3}\,\boldsymbol{\xi}^2 + \boldsymbol{\eta}^2\right), \end{aligned} \tag{62}$$

where $\omega_1 = \omega_2 = \omega_{\mathrm{d}} = \omega$, $\omega_3 = \omega_{\mathrm{u}}$, $\omega_+ = 2\omega + \omega_3$. The last chain in formula (62) corresponds to the identification of the Torricelli point $\mathbf{x}_{\mathrm{Y}}$, with the center of mass providing a good approximation for virtually equal masses. The equation for the neutron ground state, disregarding contributions from ΔM_{OGE}, ΔM_{SS}, and ΔM_{SE}, has the form

$$(\hat{H}_B + V_\sigma + V_{\mathrm{conf}})\varphi(\boldsymbol{\eta}, \boldsymbol{\xi}) = M_0(\omega_i, \gamma)\varphi(\boldsymbol{\eta}, \boldsymbol{\xi})\,. \tag{63}$$

The total baryon wave function is the product of coordinate $\varphi(\boldsymbol{\eta}, \boldsymbol{\xi})$ and spin-flavor functions. A few symmetries are simultaneously broken in an MF:

(1) states $J = 1/2$ and $J = 3/2$ are mixed;

(2) isotopic states $I = 1/2$ and $I = 3/2$ are similarly mixed;

(3) summands of the Hamiltonian H_B and V_{conf} lack symmetry with respect to inversion $\boldsymbol{\eta} \to -\boldsymbol{\eta}$.

It can be shown [81] that, in the case of switching on the MF and with regard to the above symmetry considerations, the spin-flavor function $\mathrm{d}_-\mathrm{d}_-\mathrm{u}_+$ corresponds to the lowest state. In approximation (62) for V_{conf}, equation (63) reduces to the equation for the potential in the form of the sum of potentials of two oscillators, known in quantum mechanics. The expression for the neutron dynamic mass is obtained by solving the spectral problem (63) for the three-particle generalization of Hamiltonian (39), taking into account expression (62) as well as spin and relativistic terms V_σ for the $\mathrm{d}_-\mathrm{d}_-\mathrm{u}_+$ configuration:

$$\begin{aligned} \frac{M_0}{\sqrt{\sigma}} &= \Omega_{\xi\perp} + \Omega_{\eta\perp} + \frac{1}{2}\left(\Omega_{\xi\parallel} + \Omega_{\eta\parallel}\right) + \frac{3\sqrt{\sigma}\gamma}{2} \\ &+ \frac{m_{\mathrm{d}}^2 + \omega^2 - eB/2}{\omega\sqrt{\sigma}} + \frac{m_{\mathrm{u}}^2 + \omega_3^2 - eB}{2\omega_3\sqrt{\sigma}}\,, \end{aligned} \tag{64}$$

where

$$\begin{aligned} \Omega_{\xi\perp} &= \left[\left(\frac{eB}{4\sigma}\right)^2 \frac{a_+^2}{a^2 a_3^2} + \frac{a_3^2 + 2a^2}{\beta a a_+ a_3}\right]^{1/2}, \\ \Omega_{\eta\perp} &= \left[\left(\frac{eB}{4\sigma}\right)^2 \frac{1}{a^2} + \frac{1}{\beta a}\right]^{1/2}, \\ \Omega_{\xi\parallel} &= \left(\frac{a_3^2 + 2a^2}{\beta a a_+ a_3}\right)^{1/2}, \qquad \Omega_{\eta\parallel} = \frac{1}{\sqrt{\beta a}} \end{aligned} \tag{65}$$

and notations $\omega = a\sqrt{\sigma}, \omega_3 = a_3\sqrt{\sigma}, \gamma = \beta/\sqrt{\sigma}, a_+ = 2a + a_3$ are introduced. Parameters a, a_3, and β are found from the conditions

$$\left.\frac{\partial M(\omega_i, \gamma)}{\partial \omega_i}\right|_{\omega_i = \omega_i^{(0)}} = 0, \qquad \left.\frac{\partial M_0(\omega_i, \gamma)}{\partial \gamma}\right|_{\gamma = \gamma^{(0)}} = 0\,. \tag{66}$$

The wave function is factorized in the form of the product of four oscillator functions: $\varphi(\boldsymbol{\eta}, \boldsymbol{\xi}) = \varphi_1(\eta_\perp)\varphi_2(\eta_\parallel)\psi_1(\xi_\perp)\psi_2(\xi_\parallel)$ corresponding to the motion along coordinates $\boldsymbol{\eta}$ and $\boldsymbol{\xi}$ in the plane perpendicular to the MF and along the MF. Similar to mesons, neutrons undergo compression in the plane perpendicular to the MF, whereas their characteristic size along the field is determined by string tension σ.

Thus, the involvement of pseudomomentum permits separating variables only in certain special cases. For example, electroneutrality of the system is the necessary condition for mesons, whereas an additional restriction on quark spin projections is imposed for baryons. It follows from formulas (14) and (15) that the eB/σ ratio is the dimensionless parameter characterizing hadron mass spectrum in an MF. In the strong field mode ($eB/\sigma \gg 1$), the influence of confinement in the plane orthogonal to the MF direction is markedly suppressed; this permits considering quarks moving independently in their Larmor orbits. The use of the oscillator approximation for the confining potential (53) allows the motion along the MF (determined largely by confinement) to be distinguished from the motion in the perpendicular plane. It is therefore possible to write down the sum: $M(\omega_1, \omega_2, \gamma) = M_\perp + M_3$. The independent quark approximation makes possible representation of the wave function as the product

$$\Psi(\mathbf{r}_1, \mathbf{r}_2) = \psi_1^\perp(\mathbf{r}_\perp^{(1)})\psi_2^\perp(\mathbf{r}_\perp^{(2)})\psi^z(z^{(1)} - z^{(2)})\,. \tag{67}$$

The calculated contribution from longitudinal motion is analogous to the result obtained for neutral mesons (55), namely

$$M_3 = \sqrt{\frac{4\sigma\tilde{\omega}}{\gamma}}\left(n_z + \frac{1}{2}\right) + \frac{K_z^2}{2(\omega_1 + \omega_2)}\,.$$

The oscillator potential of quark–quark interaction can be represented as

$$\begin{aligned} \left(\mathbf{r}_\perp^{(1)} - \mathbf{r}_\perp^{(2)}\right)^2 &= \left(\mathbf{r}_\perp^{(1)} - \mathbf{r}_\perp^{0}\right)^2 + \left(\mathbf{r}_\perp^{(2)} - \mathbf{r}_\perp^{0}\right)^2 \\ &- 2\left(\mathbf{r}_\perp^{(1)} - \mathbf{r}_\perp^{0}\right)\left(\mathbf{r}_\perp^{(2)} - \mathbf{r}_\perp^{0}\right) \to \sum_{i=1}^{2}\left(\mathbf{r}_\perp^{(i)} - \mathbf{r}_\perp^{0}\right)^2, \end{aligned} \tag{68}$$

where $\mathbf{r}_\perp^0$ is the position of the meson center of mass. When calculating the ground state of a compound system with potential (68), it can be assumed that the center of mass is

motionless in the xy plane and put $\mathbf{r}_\perp^0 = 0$. The assumption holds for charged mesons, because translational symmetry for the center of mass is clearly broken in an MF. For neutral mesons, equally true is the assumption of a meson resting in the ground state, because the system's energy is minimal when the pseudomomentum is $K = 0$. On the other hand, the pseudomomentum of the ground state is proportional to the center-of-mass momentum $\langle \mathbf{P} \rangle$ (56), $\langle \mathbf{K} \rangle \sim \langle \mathbf{P} \rangle$ for oscillator potential (62). Approximation (68) leads to efficient lengthening of the confinement string. To extend the scope of applicability of the constituent separation method to weak fields, $eB/\sigma < 1$, effective tension can be introduced for each part of the string, σ_1 and σ_2, connecting quarks to the center of mass as follows:

$$\sigma_1 = \frac{\sigma}{1 + \omega_1/\omega_2}\,, \qquad \sigma_2 = \frac{\sigma}{1 + \omega_2/\omega_1}\,. \tag{69}$$

The string tension 'renormalization' procedure is described at length in the Appendix to Ref. [25]. The confinement potential eventually takes the form

$$V_{\text{conf}} = \frac{\sigma_1}{2\gamma}\left(\mathbf{r}_\perp^{(1)} - \mathbf{r}_\perp^0\right)^2 + \frac{\sigma_2}{2\gamma}\left(\mathbf{r}_\perp^{(2)} - \mathbf{r}_\perp^0\right)^2 + \frac{\sigma\gamma}{2}\,. \tag{70}$$

'Renormalization' of tension σ results in the dynamic part of the neutral meson mass calculated by the CS method coinciding numerically with the mass calculated exactly with the use of the pseudomomentum (14) over the entire range of the MF of interest. The motion in plane xy makes the following contribution to the energy spectrum:

$$M_\perp = \sum_{i=1}^{2}(2n_\perp^{(i)} + 1)\Omega_i\,, \qquad \Omega_i = \frac{1}{2\omega_i}\sqrt{(e_iB)^2 + \frac{4\sigma_i\omega_i}{\gamma}}\,. \tag{71}$$

The constituent separation method is generalized in a trivial fashion for the case of a three-body system. The main advantage of the CS technique is the possibility of considering charged and neutral hadrons in a single approach. Moreover, the introduction of effective string tension permits the results obtained to be reproduced using the pseudomomentum technique with an accuracy of about 5%.

The wave function of the hadron ground state in an MF obtained by the CS method has the form

$$\Psi_0 = \left(\frac{\tilde{\omega}^{(0)}\Omega_z}{\pi}\right)^{1/4} \exp\left[-\frac{\tilde{\omega}^{(0)}\Omega_z}{2}\left(\mathbf{z}^{(1)} - \mathbf{z}^{(2)}\right)^2\right] \times \prod_{i=1}^{2}\left(\frac{\omega_i^{(0)}\Omega_i}{\pi}\right)^{1/4} \exp\left[-\frac{\omega_i^{(0)}\Omega_1}{2}\left(\mathbf{r}_\perp^{(i)}\right)^2\right]. \tag{72}$$

To recall, wave function (72) is obtained by continuous deformation of the wave function in zero MF and for zero quark angular momenta l_1 and l_2. In the superstrong magnetic field $eB/\sigma \gg 1$ and independent quark approximation, it is necessary to take into consideration the fact that the ground state is infinitely degenerate in angular momenta projections m_1 and m_2 by analogy with Landau level degeneracy for a single particle in the symmetric gauge. For this reason, wave functions need to be modified in the calculation of perturbative corrections. This problem is considered in the Appendix B to Ref. [25].

The CS method can be employed to derive analytical expressions for the asymptotic form of hadron mass trajectories in an MF. In the case of a weak MF, $eB < \sigma$, the mass can be expanded in the small parameter eB/σ to obtain

$$M_0(B) = M_0(B = 0) - \sum_{i=1}^{2}\frac{e_i\boldsymbol{\sigma}^{(i)}\mathbf{B}}{2\omega_i^{(0)}} = M_0(B = 0) - \boldsymbol{\mu}\mathbf{B} + c|e\mathbf{B}|\,, \tag{73}$$

where $\boldsymbol{\mu}$ is the magnetic moment, and item $c|e\mathbf{B}|$ corresponds to the precession energy of the charged hadron center of mass in the magnetic field (the lowest Landau level). Calculation of meson magnetic moments by the correlator method reported in Refs [85, 86] demonstrates excellent agreement with the results of lattice calculations.

The situation is more complicated in the strong magnetic field regime $eB \geqslant \sigma$. Let us first consider the case in which all quarks and antiquarks are at the lowest Landau levels, i.e., $n_\perp^{(i)} = 0$ and spin orientations $e_i\sigma_z^{(i)} = |e_i|$, $i = 1, 2$. The dynamic mass of these states tends to be constant in the $eB \to \infty$ limit. Indeed, if the dynamic mass is represented as

$$M^{\text{ZHS}} = M_0(eB \gg \sigma) = M_\perp + M_3 + \frac{\sigma\gamma}{2} \simeq M_3 + \sum_{i=1}^{2}\frac{m_i^2 + \omega_i^2}{2\omega_i} + \frac{\sigma\gamma}{2}\,, \tag{74}$$

the calculation of stationary values $\omega^{(0)} = \omega_i^{(0)} = \sqrt{\sigma}/2$, $\gamma^{(0)} = 1/\sqrt{\sigma}$ gives

$$M^{\text{ZHS}} = 2\sqrt{\sigma}\,. \tag{75}$$

A similar result for neutral mesons can be obtained by the pseudomomentum method from formula (59). We shall use the abbreviation ZHS (Zero Hadron State) to denote these states.

A different situation takes place when one of the meson quarks distorts the equality $e_i\sigma_z^{(i)} = |e_i|$. For $e_2\sigma_z^{(2)} \neq |e_2|$, the following equation holds for the ground state mass:

$$M^{\text{I}} = M_\perp^0 + M_3^0 = \frac{\omega_1}{\gamma} + \frac{\sigma}{\gamma e_1 B} + \frac{\sigma}{\gamma e_2 B} + \frac{1}{2}\sqrt{\frac{\sigma}{\tilde{\omega}\gamma}} + \frac{\omega_2^2 + 2e_2B}{2\omega_2} + \frac{\sigma\gamma}{2}\,, \tag{76}$$

which leads to the stationary values $\omega_1^{(0)} = 2^{-5/6}\sqrt{\sigma}$, $\omega_2^{(0)} = \sqrt{2e_2B}$, and $\gamma^{(0)} = 1/\sqrt{2\sigma}$. The respective asymptotic behavior is called type I:

$$M^{\text{I}} = \sqrt{2e_2B} + \sqrt{2\sigma}\,. \tag{77}$$

In the third variant, there is no single quark at the LLL, i.e., $e_i\sigma_z^{(i)} \neq |e_i|$. The stationary point calculation, in analogy with (77), yields $\omega_i^{(0)} = \sqrt{2e_iB}$, $\gamma^{(0)} = 2^{-2/3}(\sigma\tilde{\omega}^{(0)})^{-1/3}$ and respective (type II) asymptotic behavior

$$M^{\text{II}} = \sqrt{2e_1B} + \sqrt{2e_2B}\,. \tag{78}$$

In a word, all meson mass trajectories in the MF corresponding to different orientations of quark spins with respect to the field can be classified based on three types of asymptotic behavior: two growing with the MF as $\sim \sqrt{eB}$ (I and II), and the third one tending to be constant

(ZHS):

$$\text{ZHS:}\ \ e_1\sigma_z^{(1)} > 0,\ \ e_2\sigma_z^{(2)} > 0,\ \ \tilde{M}_{\rm d}^{\rm ZHS}(eB \gg \sigma) = 2\sqrt{\sigma}\,, \tag{79}$$

$$\text{I:}\ \ e_1\sigma_z^{(1)} > 0,\ \ e_2\sigma_z^{(2)} < 0,\ \ \tilde{M}_{\rm d}^{\rm I}(eB \gg \sigma) = \sqrt{2e_1B} + \sqrt{2\sigma}\,, \tag{80}$$

$$\text{II:}\ \ e_1\sigma_z^{(1)} < 0,\ \ e_2\sigma_z^{(2)} < 0,\ \ \tilde{M}_{\rm d}^{\rm II}(eB \gg \sigma) = \sqrt{2e_1B} + \sqrt{2e_2B}\,. \tag{81}$$

It was shown in Ref. [81] that the main nonperturbative contribution to the total hadron mass is supplemented by a significant (up to 30%) contribution from perturbative corrections. The influence of an MF on the perturbative corrections is considered in Section 5.

To conclude this section, one more method for accurate variable separation needs to be mentioned (see Ref. [84]). The method based on the assumption of $e_1 = e_2 = e$ and $\omega_1 = \omega_2$ describes nonphysical mesons with charges of 4/3 for $u\bar{u}$ and 2/3 for $d\bar{d}$. This model allows analytical results to be obtained and can be used for estimative calculations. The transition to the center-of-mass variables in Hamiltonian (39) is associated with cancellation of cross terms, which results in the separation of the center-of-mass and the relative motions:

$$\begin{aligned} H_{q_1\bar{q}_2} &= \frac{\mathbf{P}^2}{4\omega} + \frac{e^2}{4\omega}(\mathbf{B}\times\mathbf{R})^2 + \frac{\boldsymbol{\pi}^2}{\omega} + \frac{e^2}{16\omega}(\mathbf{B}\times\boldsymbol{\eta})^2 \\ &\quad + \frac{2m^2 + 2\omega^2 - e(\boldsymbol{\sigma}_1 + \boldsymbol{\sigma}_2)\mathbf{B}}{2\omega} + \frac{\sigma}{2}\left(\frac{\eta^2}{\gamma} + \gamma\right) \\ &\quad + V_{\rm OGE} + V_{\rm SS} + \Delta M_{\rm SE}\,. \end{aligned} \tag{82}$$

As could be expected, the charged meson center of mass performs a precessing motion. The corresponding eigenenergies are easy to calculate:

$$\begin{aligned} M_n(\omega,\gamma) &= \frac{eB}{2\omega}(2N_\perp + 1) + \sqrt{\left(\frac{eB}{2\omega}\right)^2 + \frac{2\sigma}{\omega\gamma}}\,(2n_\perp + 1) \\ &\quad + \sqrt{\frac{2\sigma}{\omega\gamma}}\left(n_\parallel + \frac{1}{2}\right) - \frac{eB}{\omega} + \frac{\sigma\gamma}{2} + \frac{m^2 + \omega^2}{\omega} \\ &\quad + \Delta M_{\rm OGE} + \Delta M_{\rm SE} + \langle a_{\rm SS}\rangle\,. \end{aligned} \tag{83}$$

5. Perturbative corrections

Section 4 presented the relativistic Hamiltonian (41) describing nonperturbative quark dynamics inside a meson, i.e., the motion in the confinement potential and external MF. In addition, the energy spectrum of this Hamiltonian was described and wave functions found for neutral and charged mesons. A similar problem was solved for a three-quark neutron (ddu). According to expression (64), the total meson mass includes, inter alia, perturbative corrections that can be calculated in the first order of the perturbation theory, if the ground state wave function is known.

The first of the corrections present in formula (64) is $\Delta M_{\rm OGE}$, arising from gluon exchange. The source of the $V_{\rm OGE}$ potential is the perturbative part of correlator (35). The matrix element $\Delta M_{\rm OGE} = \langle\varphi_0|V_{\rm OGE}|\varphi_0\rangle$ is negative; its contribution increases with the strength of the MF. It was shown in Ref. [80] that the expression

$$\Delta M_{\rm OGE} \simeq -\sqrt{\sigma}\,\ln\ln\frac{eB}{\sigma} \tag{84}$$

may serve as an estimate for massless quarks in the $eB \gg \sigma$ limit. This phenomenon is analogous to an increase in the ground state energy of a hydrogen atom in an MF, which was discussed in the Introduction. The collapse, i.e., the unlimited decrease in the meson mass, does not occur, as in the hydrogen atom. The color Coulomb potential is screened owing to the influence of the MF on the virtual quark–antiquark loops.

Let us consider in more detail the derivation of the expression for the one-gluon exchange potential in an MF. The gluon propagator with regard to vacuum polarization by quark and gluon pairs takes on the form

$$D(q) = \frac{4\pi}{q^2 - \left[g^2(\mu_0^2)/(16\pi^2)\right]\tilde{\Pi}(q)}\,, \tag{85}$$

where polarization operators of gluons and quarks in the one-loop approximation are expressed as

$$\Pi_{\rm gl}(q) = -\frac{11}{3}\,N_{\rm c}\ln\frac{|q^2|}{\mu_0^2},\quad \tilde{\Pi}_{\rm q\bar{q}}(q) = -\frac{2}{3}n_{\rm f}q^2\ln\frac{|q^2|}{\mu_0^2}, \tag{86}$$

where $n_{\rm f}$ is the number of flavors. The MF into which a gluon is placed begins to affect quark–antiquark loops inside the polarization operator $\Pi_{\rm q\bar{q}}$. In a strong field, a quark–antiquark pair can be regarded as occupying the lowest Landau level, which results in the modification of the polarization operator:

$$\frac{\alpha_{\rm s}^{(0)}}{4\pi}\,\Pi_{\rm q\bar{q}}(q) = -\frac{\alpha_{\rm s}^{(0)}n_{\rm f}|e_{\rm q}B|}{\pi}\exp\left(-\frac{q_\perp^2}{2|e_{\rm q}B|}\right)T\left(\frac{q_3^2}{4m^2}\right), \tag{87}$$

$$T(z) = -\ln\frac{(\sqrt{1+z}+\sqrt{z})}{\sqrt{z(z+1)}} + 1 = \begin{cases} \dfrac{2}{3}\,z\,, & z \ll 1\,, \\ 1\,, & z \gg 1\,. \end{cases}$$

Such a behavior reproduces, up to the $\alpha_{\rm QED} \to \alpha_{\rm s}^{(0)}n_{\rm f}/2$ substitution, that of the electron–positron polarization operator of a hydrogen atom in the MF (see Refs [34–36]). The mass parameter m in formula (87), corresponding in QED to the renormalized electron mass, is replaced by the characteristic quark–antiquark pair energy in the confinement regime, i.e., $4m^2 \to 4\sigma$. Notice the absence of the nonperturbative quark–antiquark interaction inside a virtual pair, as a consequence of the confining string topology (Fig. 1).

The final expression for the one-gluon exchange potential in the momentum representation in a strong MF [87] looks like

$$\begin{aligned} V_{\rm OGE}(Q) &= 3\alpha_{\rm s}^{(0)}\,\frac{1}{3}\left\{Q^2\left[1 + \frac{\alpha_{\rm s}^{(0)}}{4\pi}\,\frac{11}{3}N_{\rm c}\ln\left(\frac{Q^2 + M_B^2}{\Lambda_{\rm QCD}^2}\right)\right]\right. \\ &\quad \left. + \frac{\alpha_{\rm s}^{(0)}n_{\rm f}|eB|}{\pi}\exp\left(-\frac{Q_\perp^2}{2|e_{\rm q}B|}\right)T\left(\frac{Q_3^2}{4\sigma}\right)\right\}^{-1}, \end{aligned} \tag{88}$$

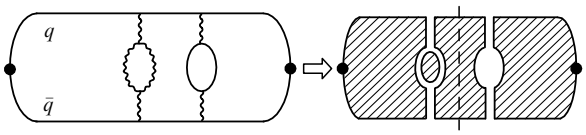

Figure 1. One-gluon exchange between a static quark and antiquark in the one-loop approximation at large $N_{\rm c}$. Hatched area corresponds to nonperturbative interaction (film of minimal area).

where $N_c = 3$, $n_f = 2$, $\alpha_s^{(0)} = 0.42$, $\Lambda_{QCD} = 0.3$ GeV, and $M_B^2 = 2\pi\sigma = 1.1$ GeV^2. The appearance of parameter M_B^2 calculated in Ref. [88] prevents the appearance of Landau singularity. Parameter M_B^2 emerges in the examination of gluon propagator $G_{gl}^{-1} = (D(B))_{ab}^2 \delta_{\mu\nu} - 2gF_{\mu\nu}^c(B) f^{abc}$ in the background stochastic field B_μ, $A_\mu = a_\mu + B_\mu$. The gluon polarization operator in the expression for the running coupling constant in averaging over the stochastic background field, namely

$$\frac{1}{g^2(Q^2)} = \frac{1}{g^2(\mu^2)} - \frac{11}{3} N_c \Pi_{gl}(Q^2, \mu^2) \tag{89}$$

can be interpreted at large N_c as an object defined by the closed double gluon line (see Fig. 1), inside which a confining string is contained in the fundamental representation. As a result, the gluon polarization operator acquires natural infrared regularization determined by the gluon loop mass M_B.

Calculation of the perturbative correction for the meson mass, resulting from one-gluon exchange, reduces to averaging the matrix element (88) over the wave function (57) of the meson ground state:

$$\Delta M_{OGE} = \langle V(Q) \rangle_{mes} = \int V(Q) \psi^2(q_\perp, q_3) \frac{d^2 q_\perp \, dq_3}{(2\pi)^3} . \tag{90}$$

Therefore, stretching the wave function into an ellipsoid of revolution with the characteristic radii $r_\perp \approx \sqrt{2/(eB)}$ and $r_3 \approx \sqrt{2/\sigma}$ no longer results in the 'color Coulomb catastrophe' (Fig. 2). The solid curve shows that the correction is included in the saturation regime in an asymptotically large magnetic field; however, it decreases in an uncontrolled manner in the absence of MF influence on virtual quark–antiquark pairs (dashed curve). In a similar way, the inclusion of quark loops ensures regularization of the contribution from one-gluon exchange to the neutron mass [81].

Spin–spin interaction $V_{SS}(r)$ originates from spin-dependent kernels $\Phi_\sigma(1)\Phi_\sigma(2)$ (see formula (25)) averaged over the stochastic vacuum gluon field $\langle \sigma_{\mu\nu}(1) F_{\mu\nu}(x) \sigma_{\rho\lambda}(2) F_{\rho\lambda}(y) \rangle$. Here, the perturbative part of the correlator stands for the relativistic spin–spin interaction:

$$V_{SS} = \frac{\alpha_s}{3\omega_1\omega_2} \left[\frac{3(\boldsymbol{\sigma}_1 \mathbf{r}_1)(\boldsymbol{\sigma}_2 \mathbf{r}_2)}{r^5} - \frac{\boldsymbol{\sigma}_1 \boldsymbol{\sigma}_2}{r^3} \right] + \frac{8\pi\alpha_s}{9\omega_1\omega_2} (\boldsymbol{\sigma}_1 \boldsymbol{\sigma}_2) \delta^{(3)}(\mathbf{r}) . \tag{91}$$

Setting $i = j$ in the correlator $\langle \sigma(i) F \sigma(j) F \rangle$ yields the nonperturbative self-energy part for each quark:

$$\Delta M_{SE}(i) = -\frac{3\sigma}{2\pi\omega_i^{(0)}} . \tag{92}$$

It follows from formula (91) that, in the case of $\omega_i \to m_i$ substitution, hyperfine interaction coincides up to a constant with spin–spin interaction in quantum mechanics. The first term (tensor forces) in Eqn (91) is disregarded in considering the meson ground state. Consideration of the Zeeman effect in the hydrogen atom placed in an MF [39] (Section 6) gives evidence that these forces become noticeable only when the wave function elongates into a needle-like shape along the superstrong MF. Averaging (91) over the meson ground-state wave function (57) reveals a weaker MF dependence than that of the term with the δ-function, which makes it possible to disregard the contribution of the tensor term. As a result, the hyperfine interaction correction assumes the form

$$\Delta M_{SS} = \frac{8\pi\alpha_s}{9\omega_1\omega_2} |\psi(0)|^2 (\boldsymbol{\sigma}_1 \boldsymbol{\sigma}_2) . \tag{93}$$

The structure of formula (93) suggests that hyperfine interaction not only makes allowance for the mass correction but also leads to the mixing of levels with different spin projections, as shown in Section 7.

Formulas (57) and (58) indicate that the wave function of the meson ground state in a strong MF is an ellipsoid of revolution. Due to the shortening of the transverse radius as $r_\perp \sim \sqrt{2/(|e|B)}$, quantity $|\psi(0)|^2 \sim eB$; i.e., it grows linearly with the strength of the MF, which inevitably leads to the uncontrolled rapid decrease in the matrix element (93). If the minus sign of the ground state is taken into account, this correction can be a cause of collapse in a magnetic field $eB \simeq 0.4$ GeV^2. This defect occurs in the first order of the perturbation theory, but the singular nature of the δ-like interaction makes impossible the consistent recording of hyperfine interaction in all orders of the perturbation theory. At the same time, the characteristic correlation length of vacuum stochastic fields over which averaging is performed in the calculation of a given matrix element is $\lambda \simeq 1$ GeV^2. Therefore, δ-interaction can be 'smeared' over the ultraviolet parameter λ using a Gaussian form factor:

$$\delta^{(3)}(\mathbf{x}) \to \left(\frac{1}{\sqrt{\pi}\lambda} \right)^3 \exp\left(-\frac{\mathbf{r}^2}{\lambda^2} \right) . \tag{94}$$

This regularization procedure results, as in the case of one-gluon exchange, in correction (93) being included in the saturation at $eB \simeq 0.4$ GeV^2, and the scenario of hyperfine interaction collapse is not realized.

In this section, we considered two possible scenarios of the collapse emergence and mechanisms to prevent them. The results agree with the general statement that eigenvalues of the relativistic Hamiltonian are invariably positive in the absence of external electric fields, which means that the MF cannot be a cause of mass spectrum instability. This theorem is considered at greater length in Section 10.

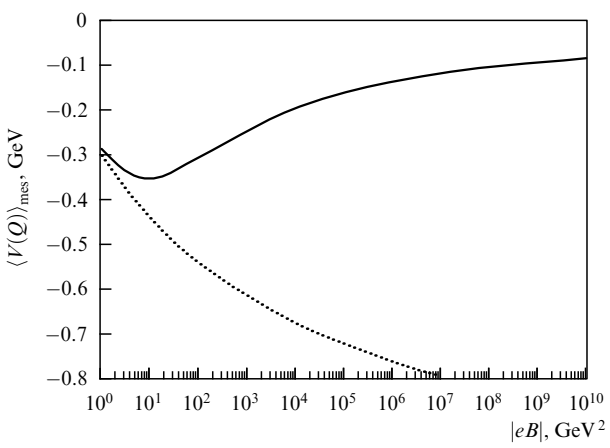

Figure 2. Contribution of one-gluon exchange to the meson mass as a function of the MF strength. Solid curve — taking into account the MF influence on $q\bar{q}$ loops; dotted curve — not taking into account the MF influence on $q\bar{q}$ loops.

6. Magnetic focusing

It was shown in Section 5 that, in an external MF comparable to the characteristic energy of pairwise particle interactions in the system, a rise in $|\psi(0)|^2$, called 'magnetic focusing' of the wave function, markedly affects perturbative corrections [39, 65]. Let us turn back to expression (13) for the Hamiltonian of a two-particle system in an MF and take notice of the diamagnetic term $e^2(\mathbf{B}\times\boldsymbol{\eta})^2/(8\mu)$ that assumes the oscillatory form $(eB)^2\rho^2/(8\mu)$. This interaction gives evidence that quantity $|\psi(0)|^2$ in an MF should increase almost linearly with the field strength, $|\psi(0)|^2 \sim (|e|B)\kappa$, where κ is the characteristic momentum of internal motion along the z-axis.

Reference [39] shows that magnetic focusing affects the frequency of the 21-cm radio line. It was mentioned in the Introduction that the energy of the hydrogen atom ground state energy in an MF logarithmically increases in absolute value. The wave function elongates in the direction of the field, and the longitudinal/transverse size ratio grows in accordance with expression (35),

$$\frac{r_\parallel}{r_\perp} \sim \frac{\sqrt{H}}{\ln H}\,, \tag{95}$$

where $H = B/B_{\rm a}$. Focusing increases the wave function value at the origin of coordinates. In the $H \gg 1$ limit, one obtains

$$\left|\psi(0)\right|^2 \sim H \ln H\,. \tag{96}$$

Deviation of the wave function from a spherical shape results in the appearance of tensor forces. This and an increase in $|\psi(0)|^2$ give rise to the correction for the 21-cm line frequency amounting in the limit of $H \gg 1$ to the following [39]:

$$\delta\nu \simeq \alpha^6\left(\frac{m_{\rm e}}{m_{\rm p}}\right)m_{\rm e}(H\ln^2 H) \simeq 10^{-6}(H\ln^2 H)\ [\text{MHz}]\,. \tag{97}$$

Factor $|\psi(0)|^2$ affects reactions in the MF involving oppositely charged particles in both the initial and final states [65]. The probability of the process in the presence of two oppositely charged particles in the final state increases in proportion to

$$\rho(eB) = \frac{w(eB)}{w(0)} \simeq \frac{|e|B}{\kappa^2}\,, \tag{98}$$

where $w(eB)$ is the phase volume in the MF, and $w(0) \sim \kappa^2$ is the two-dimensional phase volume in the absence of an MF. The major contribution to the enhancement comes from the LLL. The effect of β-decay enhancement in an MF was known earlier [89]. The influence of an MF on positronium annihilation was explored in Refs [90, 91]. Other processes in MFs were discussed in Refs [44, 45].

One more important aspect of magnetic focusing relates to the hyperfine spin–spin interaction. It was shown above following study [39] that focusing the spin–spin interaction changes the frequency of the 21-cm radio line. For QCD systems in an MF, such as mesons, the hyperfine interaction can at first sight lead to vacuum instability. To recall, spin–spin interaction viewed in the context of the perturbation theory can be represented in the form of the volume integral of an expression containing $\delta(\mathbf{r}_1 - \mathbf{r}_2)$ [73, 92]. Taking into account higher order effects smears the δ-function, which prevents a fall on the center or collapse. Section 10 presents a theorem [71] stating that an arbitrary strong MF (in the absence of external electric fields) cannot affect the stability of the hadron spectrum.

An unexpected result of magnetic focusing is anisotropy of QCD string tension. Recent lattice calculations [93–96] have demonstrated that the confinement potential $V(\mathbf{R})$ in an MF decreases in the $\mathbf{R}$ direction parallel to $\mathbf{B}$, but increases in the perpendicular direction. Direct interaction between an MF and gluon field is absent. The influence of an MF on the string is mediated through virtual quark–antiquark pairs generated by gluons in states $^3\mathrm{S}_1$ and $^3\mathrm{P}_0$. Due to magnetic focusing, pairs moving in the plane perpendicular to the MF receive an additional energy $\Delta E = 2(m_{\rm q}^2 + |e_{\rm q}B|)^{1/2}$, whereas $\Delta E = 0$ when the pairs propagate along the MF [100]. Confinement anisotropy is disregarded, since the accuracy of calculations of meson and baryon spectra in an MF made in this review is insufficient for its estimation.

7. Mixing and splitting of mass trajectories in a magnetic field

The external magnetic field breaks spin and isospin symmetry and thereby causes the splitting of levels for different spin–isospin sates of hadrons.

The relativistic Hamiltonian (39) of hadrons in an MF contains terms describing in a nonperturbative way the interaction of quark magnetic moments with magnetic fields and the perturbative correction for hyperfine interaction depending on the mutual orientation of quark spins (91).

To study the behavior of mesons with different spin projections onto the MF direction, the relativistic Hamiltonian projection can be represented in a compact form in the space of spin states:

$$\hat{M}_{\rm total} = \left[\langle\psi_0|\hat{M}(B)|\psi_0\rangle + V_{\rm OGE} + \Delta M_{\rm SE}\right]\hat{1} - \sum_{i=1}^{2}\frac{e_i\hat{\boldsymbol{\sigma}}_i\,\mathbf{B}}{2\omega_i^{(0)}} + \frac{8\pi\alpha_{\rm hf}}{9\omega_1^{(0)}\omega_2^{(0)}}\left|\psi(0)\right|^2\hat{\boldsymbol{\sigma}}_1\,\hat{\boldsymbol{\sigma}}_2\,. \tag{99}$$

After calculating stationary values for ω_i using minimization of Hamiltonian (39) for each of all possible configurations of quark spins, $|++\rangle$, $|+-\rangle$, $|-+\rangle$, $|--\rangle$, it is necessary to diagonalize expression (99) in the space of spin states. From the mathematical standpoint, this problem is analogous to the quantum-mechanical problem of the Zeeman effect.

In the absence of an MF, hadron isospin and total spin are conserved quantum numbers that can be used to classify π- and ρ-mesons, as shown in Table 1.

In the strong field regime, $eB \gg \sigma$, the third term in formula (99) responsible for the mixing of levels is small compared with the remaining ones; therefore, splitting of mass trajectories is largely determined by quark magnetic moment projections onto the MF direction. The asymptotic behavior of mass trajectories in the $eB \gg \sigma$ limit was calculated by the constituent separation method (see formulas (79)–(81)). The type of asymptotic behavior, I, II, or ZHS, for all 12 meson states is specified in the second column of Table 1.

States 1 and 2 of a ρ^+-meson are regarded as 'pure' and do not undergo mixing as the MF increases. States 3 and 4 of mesons ρ^+ ($s = 1, s_z = 0$) and π^+ in the absence of an MF are a mixture of $|\mathrm{u}\uparrow\bar{\mathrm{d}}\downarrow\rangle$ and $|\mathrm{u}\downarrow\bar{\mathrm{d}}\uparrow\rangle$ states in different propor-

Table 1. Classification of π- and ρ-mesons by the type of asymptotic behavior.

No.	Meson state	Type of asymptotic behavior
1	$\rho^+(s_z=1)=\lvert u\uparrow \bar{d}\uparrow\rangle$	ZHS
2	$\rho^+(s_z=-1)=\lvert u\downarrow \bar{d}\downarrow\rangle$	II
3	$\rho^+(s_z=0)=\frac{1}{\sqrt{2}}\left(\lvert u\uparrow \bar{d}\downarrow\rangle+\lvert u\downarrow \bar{d}\uparrow\rangle\right)$	I
4	$\pi^+(s_z=0)=\frac{1}{\sqrt{2}}\left(\lvert u\uparrow \bar{d}\downarrow\rangle-\lvert u\downarrow \bar{d}\uparrow\rangle\right)$	I
5	$\rho^0(s_z=1)=\frac{1}{\sqrt{2}}\left(\lvert u\uparrow \bar{u}\uparrow\rangle+\lvert d\uparrow \bar{d}\uparrow\rangle\right)$	I
6	$\rho^0(s_z=-1)=\frac{1}{\sqrt{2}}\left(\lvert u\downarrow \bar{u}\downarrow\rangle+\lvert d\downarrow \bar{d}\downarrow\rangle\right)$	I
7	$\rho^0(s_z=0)=\frac{1}{\sqrt{2}}\left[\frac{1}{\sqrt{2}}\left(\lvert u\uparrow \bar{u}\downarrow\rangle+\lvert d\uparrow \bar{d}\downarrow\rangle\right)+\frac{1}{\sqrt{2}}\left(\lvert u\downarrow \bar{u}\uparrow\rangle+\lvert d\downarrow \bar{d}\uparrow\rangle\right)\right]$	ZHS + II
8	$\pi^0(s_z=0)=\frac{1}{\sqrt{2}}\left[\frac{1}{\sqrt{2}}\left(\lvert u\uparrow \bar{u}\downarrow\rangle+\lvert d\uparrow \bar{d}\downarrow\rangle\right)-\frac{1}{\sqrt{2}}\left(\lvert u\downarrow \bar{u}\uparrow\rangle+\lvert d\downarrow \bar{d}\uparrow\rangle\right)\right]$	ZHS + II
9	$\rho^-(s_z=1)=\lvert d\uparrow \bar{u}\uparrow\rangle$	II
10	$\rho^-(s_z=-1)=\lvert d\downarrow \bar{u}\downarrow\rangle$	ZHS
11	$\rho^-(s_z=0)=\frac{1}{\sqrt{2}}\left(\lvert d\uparrow \bar{u}\downarrow\rangle+\lvert d\downarrow \bar{u}\uparrow\rangle\right)$	I
12	$\pi^-(s_z=0)=\frac{1}{\sqrt{2}}\left(\lvert d\uparrow \bar{u}\downarrow\rangle-\lvert d\downarrow \bar{u}\uparrow\rangle\right)$	I

tions. In a growing field, wave functions start mixing as

$$\pi^+(B),\rho^+(B) = \alpha\,\frac{\lvert u\uparrow \bar{d}\downarrow\rangle+\lvert u\downarrow \bar{d}\uparrow\rangle}{\sqrt{2}}\pm\beta\,\frac{\lvert u\uparrow \bar{d}\downarrow\rangle-\lvert u\downarrow \bar{d}\uparrow\rangle}{\sqrt{2}} \qquad (100)$$

with coefficients α and β depending on eB and hyperfine interaction constant $\alpha_{\rm hf}$. As a result, $eB\to\infty$, while $\pi_B^+(B\to\infty)=\lvert u\downarrow \bar{d}\uparrow\rangle$ and $\rho_B^+(eB\to\infty)=\lvert u\uparrow \bar{d}\downarrow\rangle$, i.e., mesons π^+ and $\rho^+(s_z=0)$ occur at $eB=0$ in equal proportions.

The situation is somewhat more complicated in the case of neutral π^0- and ρ^0-mesons. Because the isospin is clearly distorted due to different charges of u- and d-quarks, states 9–12 undergo additional double splitting; namely, mass trajectory 9, $\rho^-(s=1,s_z=1)$, is split into two branches: $\rho^-(s=1,s_z=1)(u\bar{u})$ and $\rho^-(s=1,s_z=1)(d\bar{d})$. States 10 and 12 corresponding to mesons $\rho^0(s=1,s_z=0)$ and π^0, respectively, experience not only mixing analogous to that of charged mesons but also double splitting. As a result, the pair of states of mesons π^0 and $\rho^0(s=1,s_z=0)$ at $eB=0$ gives rise to four mass trajectories and the 12 meson states at $eB=0$ listed in Table 1 give rise to 16 trajectories. The families of states 1–4, 5–8, and 9–12 in Table 1 have a similar spin structure but differ in isospin configuration. Therefore, each family contains an asymptotic form of all three types; I, II, and ZHS.

The most 'dangerous' as regards the fall on the center are ZHS states in which the nonperturbative part of the mass becomes constant in fields $eB\gg\sigma$. The behavior of these states in the $eB>\sigma$ region is largely determined by perturbative corrections that fail to cause the collapse of all ZHS states (except for the π^0-meson state) owing to the mechanisms discussed in Section 5. The π^0-meson has a small mass, $m_{\pi^0}=135$ MeV, by virtue of chiral effects. Therefore, the formal application of the results presented in Section 5 is insufficient. The influence of an MF on the chiral structure of π^0-mesons is considered at length in Section 9.

A similar situation with mixing and splitting of energy levels with different spin projections arises in the three-body problem. The mixing of neutron and Δ^0-resonance states under the influence of an MF is discussed in paper [81]. Moreover, this study showed that the color-magnetic hyperfine interaction cannot be responsible for the level splitting at $eB=0$ observed in experiment; this finding was explained in terms of the one-pion exchange mechanism, considered at a greater length in Section 8.

8. One-pion exchange in a magnetic field

The spin–spin interaction (91) discussed above cannot support the necessary splitting of mass trajectories of the neutron and Δ^0 in a zero magnetic field. It follows from Ref. [81] that the difference between neutron (n) and Δ^0-resonance masses is $6d\simeq 0.15\alpha_{\rm s}\sqrt{\sigma}\simeq 20$ MeV for $\alpha_{\rm s}=0.35$, and $6d\simeq 100$ MeV for $\alpha_{\rm s}=1.72$. On the other hand, the measured splitting of n and Δ^0 is on the order of 300 MeV. As is known [101,102], this difference can be obtained by adding the perturbative interaction $V_{\rm OPE}$ in the form of one-pion exchange. The one-pion exchange is given by the matrix element

$$V_{\rm OPE}^{(ij)}=4\pi g_{\rm qq\pi}^2\boldsymbol{\tau}(i)\boldsymbol{\tau}(j)\,\frac{\Gamma_i\Gamma_j}{\mathbf{k}^2+m_\pi^2}\left(\frac{\Lambda^2}{\Lambda^2+\mathbf{k}^2}\right)^2, \qquad (101)$$

where $\Gamma_i=\boldsymbol{\sigma}^{(i)}\mathbf{k}/(\omega_i+M_i)$, $\omega=\sqrt{\mathbf{k}^2+m_i^2}$, and $\boldsymbol{\tau}^{(i)}$ are Pauli matrices in isospin space. It can be seen that in the limit of $m_{\rm u}=m_{\rm d}=m_\pi\to 0$ the last formula gives

$$V_{\rm OPE}\sim\frac{(\boldsymbol{\sigma}_i\,\mathbf{k})(\boldsymbol{\sigma}_i\,\mathbf{k})}{\omega_i\omega_j\mathbf{k}^2}\to\frac{\boldsymbol{\sigma}_i\,\boldsymbol{\sigma}_j}{\omega_i\omega_j},$$

i.e., the operator form of this interaction in the spin space is entirely analogous to the spin–spin one: $V_{\rm OPE}\sim\boldsymbol{\sigma}^{(i)}\boldsymbol{\sigma}^{(j)}$.

Thus, it is possible to introduce, up to the form factor in expression (101), the effective hyperfine interaction constant $\alpha_{\rm hf}=\alpha_{\rm s}+\alpha_{\rm OPE}$. It is shown in Refs [101,102] that such an approach ensures correct physical splitting for n and Δ^0 levels (−471 MeV and −79 MeV, respectively).

Let us consider the influence of a strong MF on one-pion exchange by distinguishing in expression (101) contributions from meson π^0, π^+, and π^- exchanges:

$$V_{\rm OPE}^{ij}=\frac{4\pi g^2}{\omega_i\omega_j}\left[\frac{(\boldsymbol{\sigma}_i\,\mathbf{k})(\boldsymbol{\sigma}_j\,\mathbf{k})}{k^2+m_{\pi^+}^2}\,2\tau_+^i\tau_-^j+\frac{(\boldsymbol{\sigma}_i\,\mathbf{k})(\boldsymbol{\sigma}_j\,\mathbf{k})}{k^2+m_{\pi^-}^2}\,2\tau_-^i\tau_+^j+\frac{(\boldsymbol{\sigma}_i\,\mathbf{k})(\boldsymbol{\sigma}_j\,\mathbf{k})}{k^2+m_{\pi^0}^2}\,2\tau_3^i\tau_3^j\right]\left(\frac{\Lambda^2}{k^2+\Lambda^2}\right)^2. \qquad (102)$$

It was shown in Ref. [103] and in lattice calculations [104] that the masses of π^+-mesons increase with MF strength in proportion to $\sim\sqrt{eB}$. As a result, the first two addends in formula (102) are markedly suppressed for $eB\geqslant\sqrt{\sigma}$. On the other hand, the π^0-meson mass becomes somewhat smaller and tends to remain constant afterwards as eB increases.

Both effects account for a three-fold decrease in the effective one-pion interaction constant, $\alpha_{\rm OPE}(eB \gg \sigma) = (1/3)\alpha_{\rm OPE}(eB = 0)$, in the strong MF regime.

9. π^0-meson and the fall to the center — the influence of chiral effects

Pions, unlike ρ-mesons, are pseudo-Nambu–Goldstone mesons, which implies the necessity to take into consideration how chiral degrees of freedom change under the effect of a strong external MF.

The influence of an MF on chiral effects has been investigated with the use of the chiral perturbation theory, the effective chiral Lagrangian method [105–110], the Nambu–Iona-Lasinio model [111], and other theoretical tools [112–114]. Lattice calculations of chiral properties in an MF were made in Refs [104, 115–120]. The Nambu–Iona-Lasinio model predicts augmentation of the chiral condensate according to Ref. [121], referred to in the literature as magnetic catalysis (see Ref. [122]).

In the vacuum correlator method used in this review, chiral effects are described with the aid of the effective chiral Lagrangian (ECL), obtained directly from the QCD Lagrangian in the absence [123–126] and presence [127] of an MF:

$$L_{\rm ECL} = N_{\rm c}\,{\rm tr}\log\left[(\hat{D} + m_{\rm f})\hat{1} + M\hat{U}\right], \tag{103}$$

where $m_{\rm f}$ is the current quark mass, $M(x)$ is the scalar interaction (confinement), i.e., $M(x) \sim \sigma|\mathbf{x}|$ at large $|\mathbf{x}|$, and

$$\hat{U} = \exp\left({\rm i}\gamma^s\hat{\phi}\right), \qquad \hat{\phi} = \phi_a t^a. \tag{104}$$

The Dirac operator in formula (103) is defined as $\hat{D} = \gamma^\mu(\partial_\mu - {\rm i}eA_\mu)$, where $\mathbf{A} = (\mathbf{x}\times\mathbf{B})/2$. In a recent study [128], Lagrangian (103) was invoked to derive the first six terms of the standard chiral perturbation theory up to the order $O(p^4)$. Also, the ECL method was employed to obtain all standard relations of the chiral theory, including the Gell-Mann–Oakes–Rentier (GMOR) relation. The influence of an MF on the chiral condensate and GMOR relations was studied in Ref. [129], pion decay constants were calculated in Ref. [130], and the action of an MF on the pion ground state mass was explored in Refs [103,130].

Pion masses in the chiral theory can be derived from the GMOR relation connecting pion mass, the size of the chiral quark condensate, and decay constants:

$$m_\pi^2 f_\pi^2 = \bar{m}\left|\langle\bar{\rm q}{\rm q}\rangle\right|, \qquad \bar{m} = \frac{m_{\rm u} + m_{\rm d}}{2}. \tag{105}$$

It was shown in Ref. [130] that the effective chiral Lagrangian in an external MF is diagonal with respect to quark flavors. Therefore, the π^0-meson in an MF splits into two independent components, $|{\rm u}\bar{\rm u}\rangle$ and $|{\rm d}\bar{\rm d}\rangle$; a specific GMOR relation holds for each of them:

$$m^2_{\pi_{\rm u\bar u}} f^2_{\pi_{\rm u\bar u}} = m_{\rm u}\left|\langle\bar{\rm u}{\rm u}\rangle\right|, \qquad m^2_{\pi_{\rm d\bar d}} f^2_{\pi_{\rm d\bar d}} = m_{\rm d}\left|\langle\bar{\rm d}{\rm d}\rangle\right|, \tag{106}$$

while quark (chiral) condensate $\langle\bar{\rm q}{\rm q}\rangle$ can be calculated according to Ref. [123]:

$$-\langle\bar{\rm q}{\rm q}\rangle = \left\langle {\rm tr}\,\frac{1}{M + m_{\rm q} + \hat{\partial}}\right\rangle = -\big(M(0) + m\big)G^{(0)}(k = 0), \tag{107}$$

where $G^{(0)}(k)$ is the Green's function of the pseudoscalar q$\bar{\rm q}$-meson, $M(0) \simeq \sigma\lambda \simeq 0.15$ GeV, where σ is the QCD string tension, and λ is the correlation length of vacuum gluon fields. Importantly, all quantities in the effective chiral theory constructed by the correlator method are calculated in terms of $M(0) = \sigma\lambda = 0.15$ GeV and the nonchiral Green's function spectrum $G^{(0)}(k)$. The calculation of this quantity is described in Section 2. The spectral expansion of $Q^{(0)}(k)$ in eigenstates of nonchiral relativistic Hamiltonian (55) allows the expression for the quark condensate to be obtained:

$$-\langle{\rm q}\bar{\rm q}\rangle = N_{\rm c}\big(M(0) + m_i\big)\sum_{n=0}^{\infty}\frac{\left|\psi_n(0)\right|^2}{m_n}. \tag{108}$$

Expression (108) is readily generalized to the case of an external MF taking into account each quark spin projection onto the MF direction:

$$\sum_{n=0}^{\infty}\frac{\left|\psi_n(0)\right|^2}{m_n} \to \frac{1}{2}\sum_{n=0}^{\infty}\left(\frac{\left|\psi^{(+-)}_{n,i}(0)\right|^2}{m^{(+-)}_{n,i}} + \frac{\left|\psi^{(-+)}_{n,i}(0)\right|^2}{m^{(-+)}_{n,i}}\right), \tag{109}$$

where $\psi^{(\pm\mp)}_{n,i}$ is the total set of meson wave functions obtained using the nonchiral formalism, and n is the radial quantum number.

In accordance with the asymptotic behaviors (79)–(81) for the π^0-meson, $m^{-+}_{n,i}$ rapidly increase with increasing MF. Therefore, only summands with spin projection $|+-\rangle$ in formula (109) can be taken into consideration, meaning that the asymptotic behavior of the π^0-meson mass in a strong MF is described by the dependence

$$m^2_{\pi^0} = \frac{\bar{m}}{M(0)}\left(\bar{m}^{(+-)}\right)^2, \tag{110}$$

where $\bar{m}^{(+-)}$ is a mass similar to the ground state mass $m_{n,i}$ of the nonchiral pion. As shown above, the effective chiral Lagrangian is diagonal with respect to quark flavors; therefore, the π^0-meson trajectory in the MF splits into two independent trajectories, $\pi^0({\rm u}\bar{\rm u})$ and $\pi^0({\rm d}\bar{\rm d})$. The resultant mass $\pi^0({\rm u}\bar{\rm u})$ reported for the first time in Ref. [103] is presented as a function of the MF in Fig. 3. It shows that the trajectory of the π^0-meson mass calculated using the ECL (solid curve) is significantly different from the pion mass trajectory predicted by the standard chiral perturbation

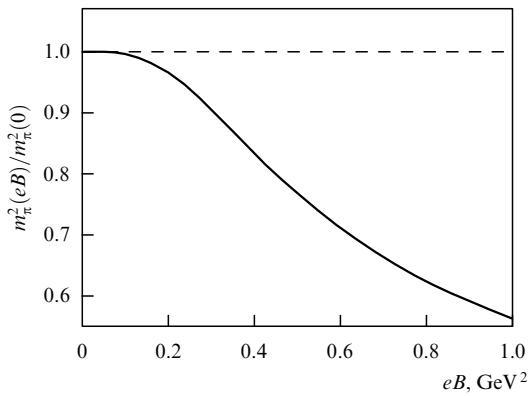

Figure 3. π^0-meson mass taking into account chiral degrees of freedom depending on MF strength (solid curve) in comparison with the prediction of the chiral perturbation theory without accounting for nonperturbative dynamics (dotted curve).

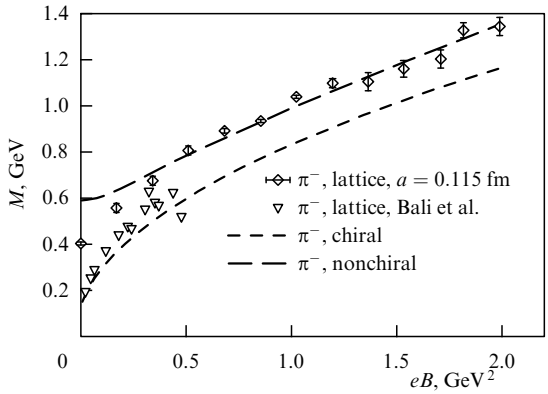

Figure 4. π^--meson mass depending on an MF taking into account chiral effects in comparison with that of the nonchiral π^--meson and results of lattice calculations [25] with lattice spacing $a = 0.115$ fm and lattice calculations of Bali et al. [131]. A charged pion loses chirality for $eB \geqslant 0{,}3\ \mathrm{GeV}^2$.

theory in the range of $eB > 0.1\ \mathrm{GeV}^2$, whereas the result obtained with the use of the ECL is in excellent agreement with that of the lattice calculations [18, 25, 48].

The situation is radically different in the case of charged π^+- and π^--mesons that lose chirality in the external magnetic field $eB > \sigma$. Their asymptotic behavior in a strong MF corresponds to type I, in accordance with the general asymptotic classification (79)–(81). Thus, the trajectory of a π^+-meson consisting of u- and $\bar{\mathrm{d}}$-quarks splits into two trajectories, depending on spin projections of individual quarks onto the MF direction: $M_{+-}(eB > \sigma) \simeq \sqrt{(2/3)eB}$ and $M_{-+}(eB \gg \sigma) = \sqrt{(4/3)eB}$, corresponding to π^+- and ρ^+-mesons, respectively. The GMOR relation yields the asymptotic behavior for the charged chiral pion:

$$M_{+-}(B) = \sqrt{m_\pi^2(0) + \frac{2}{3}\,eB}\,, \tag{111}$$

where $m_\pi^2(0)$ is the charged pion mass at $eB = 0$.

The resulting trajectories of charged π^--pions, $M_{+-}(B)$, are presented in Fig. 4, which illustrates in addition the behavior of a nonchiral π^--meson: it can be seen that the mass as $eB \to 0$ is much greater. Moreover, Fig. 4 presents results of lattice calculations [104, 131] consistent with those obtained with the use of the ECL.

In summing up this section, it can be concluded that chiral effects do not cause qualitative changes in the behavior of pseudo-Nambu–Goldstone mesons in an MF. The asymptotic behavior of the trajectories obtained in the framework of the chiral theory (see formulas (79)–(81)) remains unaltered. Importantly, consideration of chiral degrees of freedom and GMOR relations makes pion masses similar to physical ones at a near-zero MF. The growth of the chiral condensate with increasing MF is another important result obtained with the employment of the ECL in the correlator method.

10. Theorem of spectrum stability in a magnetic field

The results of analyses of the perturbative corrections in Section 5 allow the conclusion that the hadron ground state remains stable in an arbitrary strong external MF. Notice that both Coulomb and hyperfine interaction corrections also become saturated as a result of the action of quite different mechanisms; therefore, final stabilization looks like something artificial. This section is designed to discuss the general statement appeared in Ref. [71] that holds true for any QCD + QED system placed in an external MF.

Let us consider the Green's function of a fermion placed in an electromagnetic field $A_\mu^{(\mathrm{e})} = A_\mu^{(\mathrm{e})\mathrm{ext}} + a_\mu^{(\mathrm{e})}$, where $A_\mu^{(\mathrm{e})\mathrm{ext}}$ is the external background electromagnetic (EM) field and $a_\mu^{(\mathrm{e})}$ is the quantum perturbation. By analogy, for a color field we have $A_\mu = A_\mu^{\mathrm{vac}} + A_\mu$, and A_μ^{vac} is the vacuum background field. Let us start from the expression for the fermion propagator:

$$S(x,y) = (m + \hat{D})^{-1}\,, \quad D_\mu = \partial_\mu - \mathrm{i}eA_\mu^{(e)} - \mathrm{i}gA_\mu\,. \tag{112}$$

It should be emphasized that $\mu = 1, 2, 3, 4$, because the Euclidean formulation of the field theory is adopted. Then, it is assumed that both the EM and color fields are Hermitian; $(A_\mu^{(\mathrm{e})})^+ = A_\mu^{(\mathrm{e})}$ and $A_\mu^+ = A_\mu$. Real electric fields are absent; therefore, $\mathrm{i}A_0^{(\mathrm{e})} = A_4^{(\mathrm{e})} \equiv 0$. These relations are satisfied if (1) the external EM field A_μ^{ext} is Hermitian, as in the case of a purely magnetic external field, (2) vacuum color fields C_μ^{vac} are Hermitian, and (3) quantum fields C_μ and a_μ are likewise Hermitian and the space, i.e., states $|\mathrm{in}\rangle$ and $|\mathrm{out}\rangle$, contains no quanta of fields c_μ and a_μ.

Provided these conditions are fulfilled, the Green's function of the bound state for a quark–antiquark system $\mathrm{q}\bar{\mathrm{q}}$ or for the positronium can be represented in the form of the path integral performed over Euclidean quantum fields a_μ and c_μ:

$$\begin{aligned} G_{\mathrm{f}\bar{\mathrm{f}}}(x,y) &= \big\langle \mathrm{tr}\,\Gamma_1 S(x,y,A,C)\Gamma_2 S(y,x,A,C)\big\rangle \\ &= Z_{\mathrm{f}\bar{\mathrm{f}}} \int DaDcD\psi D\bar{\psi}\exp\big(-A(\psi,\bar{\psi},A,C)\big)\langle \mathrm{tr}\,\Gamma_1 S\Gamma_2 S\rangle\,, \end{aligned} \tag{113}$$

where Γ_1, Γ_2 are γ-matrices of fermions in the vertices. The fermion Green's function can be expressed using the Dirac projection operator through the scalar propagator:

$$S(x,y) = (m - \hat{D})_x (m^2 - \hat{D}^2)^{-1}_{xy}\,. \tag{114}$$

Turning back to formula (112) allows us to see that relation $(\mathrm{i}\hat{D})^+ = \mathrm{i}\hat{D}$ holds for Hermitian fields $A_\mu^{(\mathrm{e})}$ and A_μ; therefore, eigenvalues of operator $\mathrm{i}\hat{D}$ are real:

$$\mathrm{i}\hat{D}u_n = \lambda_n u_n\,, \quad \lambda_n \in \Re\,, \tag{115}$$

while eigenvalues of the squarable operator

$$-\hat{D}^2 u_n = (\mathrm{i}\hat{D})^2 u_n = \lambda_n^2 u_n\,, \quad \lambda_n^2 \geqslant 0\,, \tag{116}$$

are positively defined. It follows from the expansion of scalar propagator $(m^2 - \hat{D}^2)^{-1}$ in terms of the eigenvalues:

$$(m^2 - \hat{D}^2)^{-1} = \sum_n \frac{u_n(x)u_n^+(y)}{m^2 + \lambda_n^2}\,, \tag{117}$$

that the propagator nowhere becomes infinite. It follows from expressions (115) and (116) that operator $(-\hat{D}^2)$ is positive definite.

To recall, in the case of a composite particle consisting of fermions, eigenvalues (117) in (113) originate eventually from squarable fermion propagators. For the simplest composite particle formed from noninteracting constituents, quark

propagators can be obtained from the solution of the Dirac equation in an MF:

$$E^2 = m_q^2 + p_z^2 + (2n+1)|e|B - (eB)s_z\,, \quad s_z = \pm 1\,; \qquad (118)$$

as a result, the quark ground state has energy $E_0^2 = m_q^2$, which accounts for the absence of singularities in initial quark–antiquark Green's function (113) of the composite particle and vacuum instability. In the case of the point vector particle with spin $s = 1$ and $g = 2$ considered in Ref. [16], the initial Green's function takes the form (117) with the appropriate spectrum:

$$E^2 = m^2 + p_z^2 + (2n+1)|e|B - 2(eB)s_z\,, \quad s_z = -1, 0, +1\,, \qquad (119)$$

whence the possibility of $E^2 < 0$ for $e > 0$, $s_z = -1$ at $B = B_{\text{crit}}$. This result is a direct evidence that the description of hadron properties in an MF requires consideration of the internal structure of hadrons.

Evidently, in the presence of external electric fields ($\boldsymbol{\sigma\varepsilon} \neq 0$), the transition to Minkowski space $\boldsymbol{\sigma\varepsilon} \to \mathrm{i}\boldsymbol{\sigma\varepsilon}$ disturbs the positive definiteness of operator $m^2 - \hat{D}^2$, which gives rise to the imaginary part of Green's function $G_{\mathrm{f\bar{f}}}$ responsible for Schwinger $\mathrm{e}^+\mathrm{e}^-$-pair creation in the external electric field. The sole effect exerted by quantum electric fields in the absence of an external electric field ($\boldsymbol{\sigma\varepsilon} = 0$) is exchange processes described by Euclidean correlators:

$$e^2\langle \boldsymbol{\varepsilon}(x)\boldsymbol{\varepsilon}(y)\rangle = \frac{e^2}{\pi^2}\,\frac{1}{(x_\mu - y_\mu)^2}\,, \qquad (120)$$

$$\langle g^2 \mathbf{E}(x)\mathbf{E}(\mathbf{y})\rangle = \frac{16g^2}{3\pi^2}\,\frac{1}{(x_\mu - y_\mu)^2}\,, \qquad (121)$$

and Coulomb interaction potentials $V_{\text{Coul}} = -\alpha/r$. The main provisions of this section lead to the conclusion that a QCD + QED vacuum retains stability in any purely magnetic external field in the absence of electric fields.

11. Hadron mass trajectories in a magnetic field

In conclusion, we shall consider hadron mass spectra obtained by the vacuum correlator method. Figure 5 plots trajectories of the total mass of a neutral ρ^0-meson calculated analytically with the aid of the pseudomomentum technique for different spin configurations, taking account of perturbative corrections. Obviously, these results are in excellent agreement with the lattice calculation data [44–46]. By ρ^+ is meant a model nonphysical meson with quark charges $e_1 = e_2 = 2/3$ that allows variable separation [80].

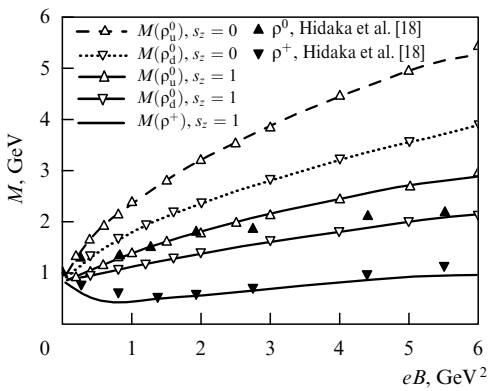

Figure 5. Mass trajectories of the ρ^0-meson calculated by the correlator method and the pseudomomentum technique in comparison with lattice calculation data [18].

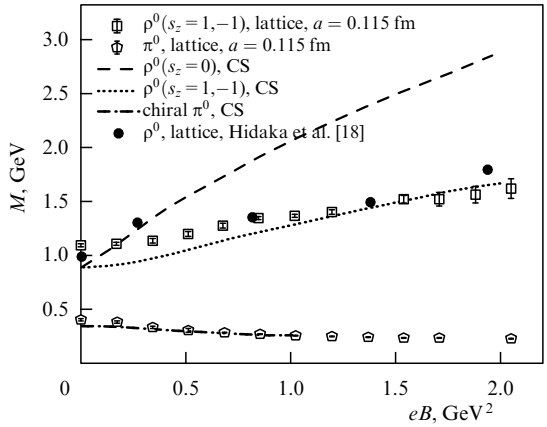

Figure 6. Mass trajectories of neutral π^0- and ρ^0-mesons made from $u\bar{u}$-quarks, which are calculated by the constituent separation (CS) method in comparison with lattice calculation data [18] (lattice spacing $a = 0.115$ fm). The result for the π^0-meson is obtained taking into account chiral effects.

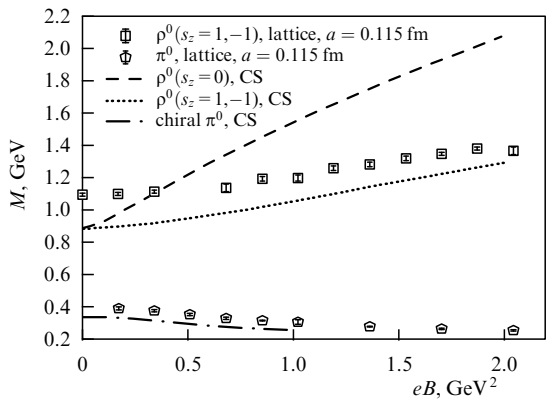

Figure 7. Mass trajectories of neutral π^0- and ρ^0-mesons made from $d\bar{d}$-quarks, which are calculated by the constituent separation (CS) method in comparison with lattice calculation data [18] (lattice spacing $a = 0.115$ fm). The result for the π^0-meson is obtained taking into account chiral effects.

The application of the constituent separation method made it possible to develop an approach allowing the simultaneous calculation of the mass spectra of both neutral and charged mesons. The crux of the method is ignoring the confinement potential in the strong field regime in the plane perpendicular to the field direction, since the light hadron behavior in an MF is characterized by the dimensionless parameter $eB/\sigma \gg 1$. This is an approximate method, in contrast to the exact analytical calculation of dynamic mass for neutral mesons using the pseudomomentum technique. A comparison of results obtained by this method for neutral mesons in $u\bar{u}$ (Fig. 6) and $d\bar{d}$ (Fig. 7) configurations with those obtained by the pseudomomentum technique (see Fig. 5) shows that the error of the CS method is about 15% for the total neutral meson mass for $eB < 0.75$ GeV^2, and about 10% in the strong field regime $eB \geqslant 0.75$ GeV^2. The

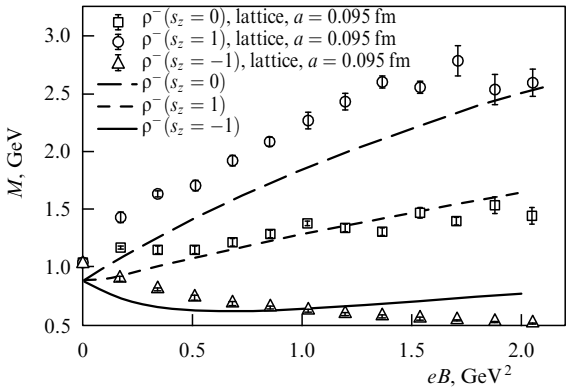

Figure 8. Mass trajectories of a charged ρ^--meson calculated by the constituent separation (CS) method in comparison with lattice calculation data.

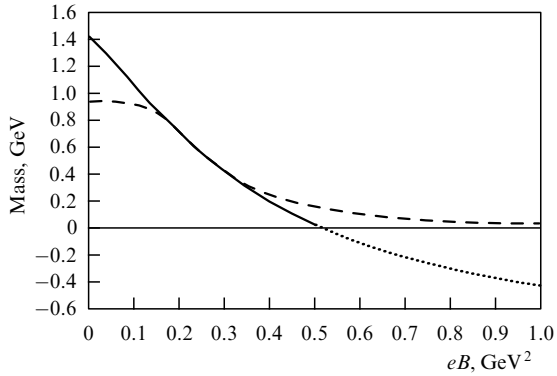

Figure 9. Neutron mass in an MF. The solid curve is a result of analytical calculation for the pure state $d_-d_-u_+$. The weak field causes Zeeman mixing of neutron and Δ^0 levels (dashed curve in the range of $0 < eB < 0.25$ GeV^2). Perturbation theory is inapplicable in the strong field region ($0.42 < eB < 0.9$ GeV^2), where the hypothetical neutron mass behavior is shown by the dashed curve.

error is mostly due to contributions of perturbative corrections to spin–spin and color Coulomb interactions calculated in the first-order perturbation theory. The next approximation is the introduction of the effective potential of a string passing through the hadron center of mass (69) that allows accurately reproducing the value of the nonperturbative part of the energy (dynamic mass) in any MF. The results for all 16 trajectories taking account of the mixing and splitting of meson spin-spin configurations (see Section 7) are presented in Figs 4, 6–8. Also, the CS method was employed to obtain analytical expressions for mass trajectory asymptotic behavior in the $eB \to \infty$ limit (79)–(81) describing the three main types of asymptotic behavior (see Table 1).

The results for ρ^+- and π^+-mesons coincide with those for ρ^-- and π^--mesons up to simultaneous reversal of the signs of quark charges and spin projections. Similar to neutral mesons, charged hadrons whose quarks occupy the lowest Landau levels (ZHS-states) are at risk of collapse when their mass starts to uncontrollably decrease and becomes negative by virtue of perturbative corrections.

This scenario is not realized for meson $\rho^-(s_z = -1)$ (and therefore for meson $\rho^+(s_z = 1)$) for the same reason as in the case of neutral mesons; namely, screening of one-gluon exchange by quark–antiquark pairs in an MF arrests the increase in the respective correction, while the magnetic focusing effect responsible for the enhancement of $|\psi(0)|^2$ and, accordingly, enhancement of spin–spin interaction is stabilized owing to the introduction of the finite correlation length of vacuum fields, $\lambda \sim 0.2$ fm, and regularization of singular δ-interaction on a given scale.

These procedures prove insufficient to prevent the collapse of the π^0-meson, it being a Nambu–Goldstone particle with a small mass at $eB = 0$ that tends to further decrease with increasing MF. Moreover, the CS method overestimates the charged π^--meson mass at $eB = 0$, if chiral degrees of freedom are disregarded (see Fig. 4). To address this problem using the vacuum correlator method, the effective chiral Lagrangian was proposed, allowing us to correctly take into consideration the pion chiral nature (see Section 9). The resulting mass trajectories of pions are presented in Figs 3, 4, showing that consideration of chiral properties makes it possible to obtain physical values for pion masses at $eB = 0$ and provides direct evidence of the absence of π^0-meson collapse in the MF. The results of calculations fairly well agree with the lattice data [18, 50, 131], which confirm the absence of collapse in the MF under consideration. Furthermore, these results are consistent with the conclusion that hadron collapse is altogether impossible in an arbitrary strong MF drawn based on the general analysis of relativistic Hamiltonian eigenvalues in an MF (see Section 10).

A qualitative analysis of the curves in Figs 6–8 shows that each of the families, $(\pi^0, \rho^0)(u\bar{u})$, $(\pi^0, \rho^0)(d\bar{d})$, (π^-, ρ^-), and (π^+, ρ^+), containing four trajectories has a single ZHS-state [79] whose dynamic mass tends to remain constant as the MF grows, two type I states increasing with the MF as $\sim \sqrt{eB}$ (80), and one type II state increasing as $\sim \sqrt{eB}$ (81). The additional double splitting of trajectories $(\pi^0, \rho^0)(u\bar{u})$ and $(\pi^0, \rho^0)(d\bar{d})$ is due to the difference between charges of u- and d- quarks responsible for the similarity of the respective mass trajectories with coefficient $\sqrt{2}$.

It is shown in Section 4 that variable separation using the pseudomomentum technique for neutrons is possible only on the assumption of $\omega_1 = \omega_2$ for d-quarks, in which case their spins must be co-directed. The mass trajectory for the respective spin–isospin configuration $|d_-d_-u_+\rangle$ taking into account perturbative corrections is presented in Fig. 9. This state has the lowest possible mass and is most vulnerable to collapse, because all the quarks occupy the LLL in the $eB \to \infty$ limit. The CS method is believed to permit mass spectra calculation for the entire baryon octet, but such work remains to be done.

It is hypothesized that a ~ 300-MeV split between neutron and Δ^0 at $eB = 0$ is due to spin–spin interaction. However, α_s playing the role of ultrafast color-magnetic interaction constant is, unlike the constant in the case of a meson, too small to ensure the experimentally obtained value for the splitting in question. The result is a ~ 35-MeV split. For this reason, Section 8 is devoted to the mechanism of one-pion exchange allowing an increase in the hyperfine interaction constant [81, 101] and ensuring the necessary splitting between n and Δ. Quantity α_{hf} introduced in this way begins to depend on the MF as the field changes masses of virtual pions, which leads to $\alpha_{hf}(eB \to \infty) \simeq (1/3)\alpha_{hf}(eB = 0)$.

The solid curve in Fig. 9 describes the dynamics of the $d_-d_-u_+$ state for which analytical calculation is possible, with the hyperfine interaction regarded in the first order of perturbation theory. The neutron wave function undergoes

Zeeman mixing with other spin configurations in the $0 < eB < 0.25\text{-GeV}^2$ range; therefore, the dashed curve corresponding to the neutron mass runs below the mass trajectory of the pure $d_- d_- u_+$ state and originates in the case of $eB = 0$ at the point corresponding to the neutron physical mass $m_n = 940$ MeV. In the range of $0.42 < eB < 0.9$ GeV^2, the dotted curve corresponds to the region in which the perturbation theory for hyperfine interaction becomes invalid, and the mass may become negative, if only the first order of the theory is taken into account. The dashed curve in the $0.42 < eB < 0.9\text{-GeV}^2$ region describes the hypothetical behavior of a neutron mass trajectory in conformity with the general stability theorem considered in Section 10.

It follows from the foregoing that analytically calculated trajectories of ρ- and π-mesons are in all cases in good agreement with the results of lattice calculations, as appears from Fig. 5 for ρ^0- and ρ^+- mesons and from Fig. 4 for the π^--meson. Of special interest is the neutron mass trajectory for which lattice calculations remain to be done. The observed discrepancies for $\rho^0(s_z = 1)$ in Fig. 7 and for $\rho^-(s_z = 1)$ in Fig. 8 can be accounted for by the low accuracy of lattice calculations.

12. Conclusions

This review deals with the problem of the influence of an MF on hadrons in the most general relativistic case when the fields can be either arbitrary strong or weak compared with the characteristic scales of the system. This required the use of the relativistic path integral in the Fock–Feynman–Schwinger representation. The relativistic Hamiltonian used in concrete calculations of energies and wave functions is actually the sole means in the case of strong interaction with confinement, since the standard methods based on the Bethe–Salpeter equation cannot be directly employed outside the framework of the perturbation theory. The RH method for hadrons is convenient to use for both weak fields ($eB \ll \sigma$), where it predicts the magnetic moments of hadrons with an accuracy of roughly 5% [85, 86], and strong fields ($eB \gg \sigma$), as shown in the present review.

Much attention was given to analytical methods of solving the spectral problem for nonrelativistic (Section 2) and relativistic (Section 4) Hamiltonians in an MF. It was shown that the introduction of pseudomomentum permits distinguishing the center-of-mass motion for electroneutral systems in an MF. The constituent separation method is proposed to consider both charged and neutral hadrons using a single formalism with the possibility of reproducing exact results for mass spectra obtained by the pseudomomentum technique in the framework of the CS method to within 10–15% over the entire range of magnetic fields being considered. The most interesting application of the CS method may be the calculation of the mass spectra of all particles making up the baryon octet in an MF and the comparison of MF effects on neutron and proton masses.

Different stages of the dynamics evolution in atomic and hadronic systems are worth mentioning. In the former systems, it is possible to distinguish a critical field $eB_a = \alpha^2 m_e^2$ and $B_{cr} = \alpha^2 B_a$ that induces electron relativistic motion, as well as the quantity $(3\pi/\alpha)B_{cr}$ at which radiative corrections freeze the rise in the binding energy, whereas in the latter case the critical field value is $eB_\sigma = \sigma = 0.18$ GeV$^2 \simeq 10^{19}$ G. As a result, quarks propagating in the plane perpendicular to the direction of large fields **B** perform individualized movements.

It was shown in the review that such motion is of critical importance for solving the problem of so-called ρ-collapse [16] based on the notion of the elementary nature of the ρ-meson.

Moreover, we demonstrated two more possible scenarios of collapse in an MF: (1) collapse due to one-gluon exchange, and (2) collapse resulting from hyperfine interaction, and their successful resolution. In the former case, it was shown that virtual quark loops affected by the magnetic field screen the one-gluon potential and cause its saturation; in the latter one, 'smearing' of hyperfine interactions related to the presence of higher orders should be taken into consideration, as confirmed by the theorem of vacuum stability in an MF.

The problem of meson mass trajectories in an MF is complicated by the intricate QCD dynamics that require consideration of spin and isospin degrees of freedom. Section 4 describes trajectories of three types (I, II, and ZHS); trajectories of certain mesons split into two and even four lines.

Of special interest is chiral meson physics in MFs, bearing in mind that strong fields are known to affect individual quarks, while the standard chiral theory considers a chiral meson to be a whole entity disregarding its quark nature. It was shown in this review that the standard chiral perturbation theory is not applicable to $\pi^\pm$- and π^0-mesons; the early chiral theory (ECL) [123–126] generalized in paper [103] taking into account the MF finds application for π^0-mesons. The validity of the theory is confirmed by its conformity with results of lattice calculations.

Apart from the theory and phenomena related to hadrons, the review treated some general topics, such as a phenomenon called by the authors 'magnetic focusing', which had been observed earlier by different researchers in atomic, molecular, and hadronic systems but remained unnamed and unexplored. The essence of this phenomenon is the enhancement of the wave function and convergence of oppositely charged components of the system in a growing MF, as exemplified by the frequency shift in the 21-cm radio line of a hydrogen atom and the enhancement of interaction in the final state proportional to the MF [see Eqn (98)].

An important aspect of the review is the investigation of neutrons in MFs using all available approaches and bearing in mind the key role played by the color-magnetic hyperfine interaction and pion exchange interaction (apart from confinement forces and gluon exchanges) in neutron systems. All these interaction components change with MF variation. The resultant neutron mass trajectory is presented in Fig. 9, but the region in the MF higher than 0.5 GeV^2 remains conjectural, because it strongly depends on the behavior of the hyperfine interaction.

In general, the studies discussed in this review taken together only slightly open a window to the previously unexplored world. In fact, we learned how to describe phenomena with strong interactions in an MF with an accuracy of up to 5–10% and created the relativistic apparatus making it possible to further improve the accuracy, but the area of its application can be very wide, including atoms, hadrons, nuclei, and even neutron stars, to say nothing of noncentral nucleus–nucleus collisions and the resulting quark–gluon plasma. All these problems await further research and new reviews.

Acknowledgment
The study was supported by the Russian Science Foundation (grant No. 16-12-10414).

References

1. Kharzeev D E et al., in *Strongly Interacting Matter in Magnetic Fields* (Lecture Notes in Physics, Vol. 871, Eds D Kharzeev) (Berlin: Springer, 2013) p. 1
2. Andersen O, Naylor W R, Tranberg A *Rev. Mod. Phys.* **88** 025001 (2016)
3. Miransky V A, Shovkovy I A *Phys. Rep.* **576** 1 (2015)
4. Kharzeev D E, McLerran L D, Warringa H J *Nucl. Phys. A* **803** 227 (2008)
5. Skokov V V, Illarionov A Yu, Toneev V D *Int. J. Mod. Phys. A* **24** 5925 (2009)
6. Toneev V, Rogachevsky O, Voronyuk V *Eur. Phys. J. A* **52** 264 (2016)
7. Potekhin A Y *Phys. Usp.* **53** 1235 (2010); *Usp. Fiz. Nauk* **180** 1279 (2010)
8. Harding A K, Dong Lai *Rep. Prog. Phys.* **69** 2631 (2006)
9. Schwinger J *Phys. Rev.* **82** 664 (1951)
10. Schramm S, Müller B, Schramm A J *Mod. Phys. Lett. A* **07** 973 (1992)
11. Luschevskaya E V, Solovjeva O E, Teryaev O V *J. High Energ. Phys.* **2017** 142 (2017)
12. Samsonov A *JHEP* (12) 061 (2003)
13. Aliev T M, Özpineci A, Savci M *Phys. Lett. B* **678** 470 (2009)
14. Gudiño D G, Sánchez G T *Int. J. Mod. Phys. A* **30** 1550114 (2015)
15. Braguta V V, Onishenko A I *Phys. Rev. D* **70** 033001 (2004)
16. Chernodub M N *Phys. Rev. D* **82** 085011 (2010)
17. Chernodub M N, Van Doorsselaere J, Verschelde H *Phys. Rev. D* **85** 045002 (2012)
18. Hidaka Y, Yamamoto A *Phys. Rev. D* **87** 094502 (2013)
19. Vafa C, Witten E *Nucl. Phys. B* **234** 173 (1984)
20. Chernodub M N *Phys. Rev. D* **86** 107703 (2012)
21. Chernodub M N *Phys. Rev. D* **89** 018501 (2014)
22. Li C, Wang Q *Phys. Lett. B* **721** 141 (2013)
23. Braguta V V et al. *Phys. Lett. B* **718** 667 (2012)
24. Luschevskaya E V et al. *JETP Lett.* **101** 674 (2015); *Pis'ma Zh. Eksp. Teor. Fiz.* **101** 750 (2015)
25. Andreichikov M A et al. *J. High Energ. Phys.* **2017** 7 (2017)
26. Weinberg S *The Quantum Theory of Fields* Vol. 2 (Cambridge: Cambridge Univ. Press, 1996)
27. Savvidy G K *Phys. Lett. B* **71** 133 (1977)
28. Matinyan S G, Savvidy G K *Nucl. Phys. B* **134** 539 (1978)
29. Nielsen N K, Olesen P *Nucl. Phys. B* **144** 376 (1978)
30. Ambjørn J, Olesen P *Nucl. Phys. B* **315** 606 (1989)
31. Skalozub V V *Sov. J. Nucl. Phys.* **43** 665 (1986); *Yad. Fiz.* **43** 1045 (1986)
32. Simonov Yu A *Phys. Usp.* **39** 313 (1996); *Usp. Fiz. Nauk* **166** 337 (1996)
33. Kuz'menko D S, Simonov Yu A, Shevchenko V I *Phys. Usp.* **47** 1 (2004); *Usp. Fiz. Nauk* **174** 3 (2004)
34. Schiff L I, Snyder H *Phys. Rev.* **55** 59 (1939)
35. Popov V S, Karnakov B M *Phys. Usp.* **57** 257 (2014); *Usp. Fiz. Nauk* **184** 273 (2014)
36. Vysotsky M I, Godunov S I *Phys. Usp.* **57** 194 (2014); *Usp. Fiz. Nauk* **184** 206 (2014)
37. Landau L D, Lifshitz E M *Quantum Mechanics. Non-Relativistic Theory* (Oxford: Pergamon Press, 1977); Translated from Russian: *Kvantovaya Mekhanika. Nerelyativistskaya Teoriya* (Moscow: Fizmatlit, 2016)
38. Shabad A E, Usov V V *Phys. Rev. D* **77** 025001 (2008)
39. Andreichikov M A, Kerbikov B O, Simonov Yu A *JETP Lett.* **99** 246 (2014); *Pis'ma Zh. Eksp. Teor. Fiz.* **99** 286 (2014)
40. Eides M I, Grotch H, Shelyuto V A *Phys. Rep.* **342** 63 (2001)
41. Fock V *Phys. Z. Sowjetunion* **12** 404 (1937)
42. Ritus V I *Ann. Physics* **69** 555 (1972)
43. Dong Lai *Rev. Mod. Phys.* **73** 629 (2001)
44. Johnson B R, Hirschfelder J O, Yang K-H *Rev. Mod. Phys.* **55** 109 (1983)
45. Ternov I M, Zhukovskii V Ch, Borisov A V *Kvantovye Protsessy v Sil'nom Vneshnem Pole* (Quantum Processes in a Strong External Field) (Moscow: Izd. Mosk. Univ., 1989)
46. Kuznetsov A, Mikheev N *Electroweak Processes in External Electromagnetic Fields* (New York: Springer, 2003)
47. Larina O, Luschevskaya E, Kochetkov O *PoS* **214** 120 (2014); Luschevskaya E V et al., arXiv:1411.0730; Luschevskaya E V, Larina O V *Nucl. Phys. B* **884** 1 (2014)
48. Luschevskaya E V et al. *Nucl. Phys. B* **898** 627 (2015)
49. Bali G S et al. *J. High Energ. Phys.* **2012** 044 (2012)
50. Bali G S et al. *Phys. Rev. D* **97** 034505 (2018)
51. Alford J, Strickland M *Phys. Rev. D* **88** 105017 (2013)
52. Zang R, Fu W, Liu Y *Eur. Phys. J. C* **76** 307 (2016)
53. Taya H *Phys. Rev. D* **92** 014038 (2015)
54. Liu H, Yu L, Huang M *Phys. Rev. D* **91** 014017 (2015)
55. Volkov M K, Radzhabov A E *Phys. Usp.* **49** 551 (2006); *Usp. Fiz. Nauk* **176** 569 (2006)
56. Hattori K, Kojo T, Su N *Nucl. Phys. A* **951** 1 (2016)
57. Ghosh S et al. *Phys. Rev. D* **84** 094043 (2016)
58. Lamb W E (Jr.) *Phys. Rev.* **85** 259 (1952)
59. Gor'kov L P, Dzyaloshinskii I E *Sov. Phys. JETP* **26** 449 (1968); *Zh. Eksp. Teor. Fiz.* **53** 717 (1967)
60. Avron J E, Herbst I W, Simon B *Ann. Physics* **114** 431 (1978)
61. Grotch H, Hegstrom R A *Phys. Rev. A* **4** 59 (1971)
62. Herold H, Ruder H, Wunner G *J. Phys. B* **14** 751 (1981)
63. Simonov Yu A *Phys. Lett. B* **719** 464 (2013)
64. Schmelcher P, Cederbaum L S *Phys. Rev. A* **43** 287 (1991)
65. Simonov Yu A *Phys. Rev. D* **88** 093001(2013)
66. Shabad A E, Usov V V *Phys. Rev. Lett.* **96** 189401 (2006)
67. Simonov Yu A *Nucl. Phys. B* **307** 512 (1988)
68. Simonov Yu A, Tjon J A *Ann. Physics* **228** 1 (1993)
69. Simonov Yu A, Tjon J A *Ann. Physics* **300** 54 (2002)
70. Simonov Yu A *Phys. Rev. D* **88** 025028 (2013)
71. Simonov Yu A *Phys. Rev. D* **88** 053004 (2013)
72. Simonov Yu A *Phys. Rev. D* **90** 013013 (2014)
73. Akhiezer A I, Berestetskii V B *Quantum Electrodynamics* (New York: Intersci. Publ., 1965); Translated from Russian: *Kvantiovaya Elektrodinamika* (Moscow: Nauka, 1969)
74. Makeenko Yu M *Sov. Phys. Usp.* **27** 401 (1984); *Usp. Fiz. Nauk* **143** 161 (1984)
75. Simonov Yu A, in *Perturbative and Nonperturbative Aspects of Quantum Field Theory* (Lecture Notes in Physics, Vol. 479, Eds H Latal, W Schweiger) (Berlin: Springer, 1997) p. 139
76. Simonov Yu A *Phys. Atom. Nucl.* **58** 107 (1995); *Yad. Fiz.* **58** 113 (1995)
77. Simonov Yu A, in *QCD: Perturbative or Nonperturbative? Proc. of the XVII Autumn School, 29 September – 4 October 1999, Lisboa, Portugal* (Eds L S Ferreira, P Nogueira, J I Silva-Marcos) (Singapore: World Scientific, 2001)
78. Dosch H G, Simonov Yu A *Phys. Lett. B* **205** 339 (1988)
79. Di Giacomo A, Dosch H G, Shevchenko V I, Simonov Yu A *Phys. Rep.* **372** 319 (2002)
80. Andreichikov M A, Kerbikov B O, Orlovsky V D, Simonov Yu A *Phys. Rev. D* **87** 094029 (2013)
81. Andreichikov M A, Kerbikov B O, Orlovsky V D, Simonov Yu A *Phys. Rev. D* **89** 074033 (2014)
82. Takahashi T T et al. *Phys. Rev. Lett.* **86** 18 (2001)
83. Takahashi T T et al. *Phys. Rev. D* **65** 114509 (2002)
84. Bornyakov V G et al. *Phys. Rev. D* **70** 054506 (2004)
85. Badalian A M, Simonov Yu A *Phys. Rev. D* **87** 074012 (2013)
86. Kerbikov B O, Simonov Yu A *Phys. Rev. D* **62** 093016 (2000)
87. Andreichikov M A, Orlovsky V D, Simonov Yu A *Phys. Rev. Lett.* **110** 162002 (2013)
88. Simonov Yu A *Phys. Atom. Nucl.* **74** 1223 (2011); *Yad. Fiz.* **74** 1252 (2011)
89. Kouzakov K A, Studenikin A I *Phys. Rev. C* **72** 015502 (2005)
90. Carr S, Sutherland P *Astrophys. Space Sci.* **58** 83 (1978)
91. Mills A P (Jr.) *Phys. Rev. A* **41** 502 (1990)
92. De Rújula A, Georgi H, Glashow S L *Phys. Rev. D* **12** 147 (1975)
93. Bonati C et al. *Phys. Rev. D* **89** 114502 (2014)
94. Bonati C et al. *Nuovo Cimento C* **38** 11 (2015)
95. Bonati C et al. *PoS* **214** 351 (2015)
96. Bonati C et al. *Phys. Rev. D* **92** 054014 (2015)

97. Bonati C et al. *Phys. Rev. D* **94** 094007 (2016)
98. Bonati C et al. *PoS* **256** 346 (2017)
99. Bonati C et al. *EPJ Web Conf.* **137** 03005 (2017)
100. Simonov Yu A, Trusov M A *Phys. Lett. B* **747** 48 (2015)
101. Simonov Yu A, Tjon J A, Weda J *Phys. Rev. D* **65** 094013 (2002)
102. Weda J, Simonov Yu A, Tjon J A, in *Few-Body Problems in Physics'02. Proc. of the XVIIIth European Conf. on Few-Body Problems in Physics, Bled, Slovenia, September 8 – 14, 2002* (Few-Body Systems, Supplement 14, Eds R Krivec) (Wien: Springer, 2003) p. 57
103. Orlovsky V D, Simonov Yu A *J. High Energ. Phys.* **2013** 136 (2013)
104. Bali G S et al. *Phys. Rev. D* **86** 071502(R) (2012)
105. Shushpanov I, Smilga A V *Phys. Lett. B* **402** 351 (1997)
106. Agasian N O, Shushpanov I A *Phys. Lett. B* **472** 143 (2000)
107. Agasian N O *Phys. Lett. B* **488** 39 (2000)
108. Andersen J O *Phys. Rev. D* **86** 025020 (2012)
109. Andersen J O *J. High Energ. Phys.* **2012** 5 (2012)
110. Cohen T O, McGady D A, Werbos E S *Phys. Rev. C* **76** 055201 (2007)
111. Gatto R, Ruggieri M *Phys. Rev. D* **83** 034016 (2011)
112. Agasian N O, Fedorov S M *Phys. Lett. B* **663** 445 (2008)
113. Fraga E S, Mizher A J *Nucl. Phys. A* **820** 103c (2009)
114. Fraga E S, Palhares L F *Phys. Rev.* **86** 016008 (2012)
115. Buividovich P V et al. *Phys. Lett. B* **682** 484 (2010)
116. Braguta V et al. *PoS* **2010** 190 (2010); *Phys. Atom. Nucl.* **75** 488 (2012); *Yad. Fiz.* **75** 524 (2012)
117. D'Elia M, Mukherjee S, Sanfilippo F *Phys. Rev. D* **82** 051501(R) (2010)
118. D'Elia M, Negro F *Phys. Rev. D* **83** 114028 (2011)
119. D'Elia M, in *Strongly Interacting Matter in Magnetic Fields* (Lecture Notes in Physics, Vol. 871, Eds D Kharzeev et al.) (Berlin: Springer, 2013) p. 181
120. Ilgenfritz E-M et al. *Phys. Rev. D* **85** 114504 (2012)
121. Gusynin V P, Miransky V A, Shovkovy I A *Phys. Rev. Lett.* **73** 3499 (1994)
122. Shovkovy I A, in *Strongly Interacting Matter in Magnetic Fields* (Lecture Notes in Physics, Vol. 871, Eds D Kharzeev et al.) (Berlin: Springer, 2013) p. 13
123. Simonov Yu A *Phys. Rev. D* **56** 094018 (2002)
124. Simonov Yu A *Phys. Atom. Nucl.* **67** 846 (2004); *Yad. Fiz.* **67** 868 (2004)
125. Simonov Yu A *Phys. Atom. Nucl.* **67** 1027 (2004); *Yad. Fiz.* **67** 1050 (2004)
126. Fedorov S M, Simonov Yu A *JETP Lett.* **78** 57 (2003); *Pis'ma Zh. Eksp. Teor. Fiz.* **78** 67 (2003)
127. Simonov Yu A, arXiv:1509.06930
128. Simonov Yu A *Int. J. Mod. Phys. A* **31** 1650104 (2016)
129. Simonov Yu A *J. High Energ. Phys.* **2014** 118 (2014)
130. Simonov Yu A *Phys. Atom. Nucl.* **79** 419 (2016); *Yad. Fiz.* **79** 277 (2016)
131. Bali G S et al., in *33rd Intern. Symp. on Lattice Field Theory, Lattice 2015, 14 – 18 July 2015, Kobe, Japan*; arXiv:1510.03899